

# Investigating the effect of the defrost cycles of air-source heat pumps on their electricity demand in residential buildings

George Milev<sup>a</sup>, Amin Al-Habaibeh<sup>a,\*</sup>, Simon Fanshawe<sup>b</sup>, Francesco Luke Siena<sup>a</sup>

<sup>a</sup> The Product Innovation Centre, Nottingham Trent University, Nottingham, UK

<sup>b</sup> Gannet Ltd, Nottingham, UK

## ARTICLE INFO

### Keywords:

Heat pumps  
Simulation  
Modelling  
Defrost cycles  
Grid  
Energy

## ABSTRACT

With the goal to reach net zero carbon emission, countries around the world are expected to switch from fossil fuel to more eco-friendly alternatives. This suggests that heating, transport, and energy sectors will be more dependent on electricity. Heat pump technology is expected to be the most common and clean technology to be used for heating in buildings due to its Coefficient of Performance. Air-source heat pumps are the most common type due to their ease of installation. This paper investigates how different climates around the world would affect the air-source heat pump electricity consumption and its defrost cycles; and hence the potential overall effect on the grid. A novel heat pump simulation model has been developed to understand the behaviour of the heat pump in cold weather scenarios. An experimental validation has been implemented to ensure the accuracy of the simulation model. Global case studies of cities from around the world including Amsterdam, Copenhagen, Helsinki, Stockholm, Vancouver, Ruse, Moscow, Reykjavik, Harbin and Nottingham are selected to assess the defrost cycles of air source heat pumps. The innovation of this research is in the in-depth investigation of heat pump defrost cycles. Electrifying the heating sector is expected to increase electricity consumption significantly, especially in cold weather. A detailed case study of the UK is presented with heat pumps and the examination of the impact this would have on the electricity grid is presented. Heating demands for buildings in cold weather was also simulated to calculate the required heating demand. The results show that the wide implementation of heat pumps in the UK, for example, would increase the total daily demand of electricity by approximately 144% relative to the present level of grid energy demand. In addition, the average daily energy consumption would increase by roughly 106% over the cold season. The findings are critical, and the novel methodology is applicable to many countries on global level in relation to the future effect of heat pumps on the grid and predicting the power demand needed by the additional heat pumps based on geographical location, u-values of building elements, and heating demand. It is crucial for a household to improve the insulation of their dwelling as this could considerably reduce the power demand by the heat pump and therefore the overall electricity consumption. This paper aims to inform future technology developers and policy makers regarding the expected effect of heat pump technology on the grid and the possible sudden peaks in demand.

## 1. Introduction

With the growth of the world's population, the rise of energy demand and the emitted carbon emissions have significantly increased. To date, countries around the world have been able to keep up with the demand, but it is expected to increase by 2.2 % per year until 2035 [1]. Many countries have introduced targets to achieve net-zero carbon emissions; and in November 2022, Egypt hosted in Sharm El Sheikh COP27 in order to keep the climate under control. And many countries around the world are investing in district heating and encouraging the use of electric cars

in an attempt to reach net zero. For example, in the UK the targets have been implemented into laws that are divided into two main stages. The first is dedicated to the banning of the sale of new petrol, diesel, and hybrid cars in the UK. The initial date of the ban was 2040, but this was brought forward to 2035 [2]. The second stage is to cut greenhouse gas emissions by 2050 completely compared to the levels set in 1990 [3]. Currently, the UK is halfway to its target, with a fall of around 51 % of greenhouse gas (GHG) emissions below the 1990 levels [3]. Additional changes that would be required to meet the net-zero target include proper resource and energy efficiency management and carbon capture and storage, involving bioenergy and probably hydrogen for electricity

\* Corresponding author.

E-mail address: [amin.al-habaibeh@ntu.ac.uk](mailto:amin.al-habaibeh@ntu.ac.uk) (A. Al-Habaibeh).

<https://doi.org/10.1016/j.enbuild.2023.113656>

Received 15 December 2022; Received in revised form 14 April 2023; Accepted 17 October 2023

Available online 20 October 2023

0378-7788/© 2023 The Author(s). Published by Elsevier B.V. This is an open access article under the CC BY-NC-ND license (<http://creativecommons.org/licenses/by-nc-nd/4.0/>).

Nomenclature			
<i>Equation nomenclature</i>		$Q_{ice-rem}$	Energy needed to melt the ice layer [kJ]
A	Area [m <sup>2</sup> ]	$Q_r$	Recommended hot water thermal capacity [kW]
$A_{evp}$	Area of outdoor heat exchanger [m <sup>2</sup> ]	$S_a$	Evaporator air velocity [m/s]
$A_{ts}$	Thermal storage area [m <sup>2</sup> ]	$\Delta T$	Temperature difference [K]
ACH	Air change rate of the house [air changes/hour]	$t$	time [s]
$C_{hlc}$	Contribution to heat losses coefficient [W/K]	$T_a$	Ambient temperature [K]
COP	Coefficient of performance	$T_s$	Surface temperature [K]
$C_{p_w}$	Specific heat of water [kJ/kg.K]	$U$	Heat transfer coefficient through material (U-value) [W/m <sup>2</sup> .K]
$h$	Enthalpy [kJ/s]	$U_{ts}$	Thermal storage U-value [W/m <sup>2</sup> .K]
HR	Humidity ratio [kg/kg]	$V_h$	Volume of the house [m <sup>3</sup> ]
$\dot{m}$	Mass flow rate [kg/s]	$V_{hx}$	Heat exchanger volume [m <sup>3</sup> ]
$m_{ice}$	Mass of frost layer [kg]	$V_{ice}$	Volume of frost layer [m <sup>3</sup> ]
$P_{com}$	Compressor power rating [kW]	$V_{sp}$	Specific volume [m <sup>3</sup> /kg]
$P_{sh}$	Heat pump power demand for space heating [kW]	$V_{sw1}$	Swept volume of the compressor [m <sup>3</sup> /s]
$Q_{ev}$	Evaporator capacity [kW]	$V_{ts}$	Thermal storage volume [m <sup>3</sup> ]
$Q_c$	Condenser heating capacity [kW]	$\delta_{ice}$	Frost layer thickness [mm]
$Q_{hw}$	Required heat for the thermal storage [kWh]	$\Delta T$	Temperature difference [K]
$Q_{HPout}$	Heat pump heat output capacity [kW]	$\rho_{air}$	Density of air [kg/m <sup>3</sup> ]
$Q_{iceremove}$	Energy needed to melt the ice layer [kJ]	$\rho_{ice}$	Density of frost [kg/m <sup>3</sup> ]
		$\rho_w$	Density of water [kg/m <sup>3</sup> ]

generation [4,5]. To meet the targets, some countries are promoting the implementation of electric cars and heat pumps, which are considered a greener alternative compared to their counterparts [6].

Another challenge that could occur in a future scenario is the electrification of the heating and transport sectors. Due to the expected ban of conventional cars around the world, progressively more people will likely look for alternatives such as electric vehicles. In addition, the heat pumps' popularity is steadily growing, and more households would likely prefer that option for heating their home. Heat pumps have higher efficiency and deliver considerably more heat compared to electrical resistant heaters; they also consume less energy compared to gas boilers. It is also important to note that HPs are more eco-friendly compared to gas boilers. The recent global increase in gas prices in 2022 have also enhanced the potential future demand for heat pumps. The key question though to consider is how the electricity required by the heat pumps gets produced and managed. This is not only related to simply increasing the capacity of the power stations, but also to the grid loads and the peaks that may occur throughout the day or year. Sudden peaks or drops in demand could cause a considerable strain on the voltage and frequency of the grid, which could lead to outages. It is very likely many heat pump units could undergo a defrost cycle within an overlapping time in cold weather, which could lead to high stress on the electricity network if auxiliary elements are used. This will require efficient management to ensure such situations are avoided. Heat pump technology has existed for more than a century and there has been significant research and improvements involved. Some of the state-of-the-art includes high temperature heat pumps. This technology aims to increase the performance by providing high evaporation and condensation temperatures. In a such study, a simulation and experimental work was done involving a high-temperature heat pump where the COP of the unit ranged from 3.64 to 4.87. The experiment and simulation showed similar results, and the errors were within 5 per cent [7]. The main reason for the slight difference between experimental and simulated values were due to external leakage between suction and discharge lines in the compressor in the experimental work [7]. In another study, a tri-generation system of a ground-source heat pump coupled with Photovoltaic-thermal panel was developed [8]. The aim was to cope with three energy demands simultaneously: cooling, heating and electricity. In the study the researchers performed experimental, and simulation work using TRNSYS 18, and their analysis indicated slight difference between experimental and simulation data [8]. In a similar study, a long period simulation was

performed of ground source heat pump assisted with a Photovoltaic thermal-road-collector instead of just photovoltaic thermal one. One of the aims was to find the optimal ground heat exchanger length, number of boreholes and their depth, and the minimum area of the PV thermal road collectors, where the heat pump can meet the power consumption. It was revealed that for a 10-year simulation through mathematical modelling and experimental work, the system and heat pump COP were 2.31 and 5.59 respectively. The research also found the optimal length of the ground heat exchanger to be 4000 m with 25 boreholes of depth 100 m, and PV area of 216 m<sup>2</sup> [9]. Solar thermal energy assisted heat pumps have become very popular for providing hot water and space heating in many European countries. In Denmark, for example, a simulation model of an air-to-water heat pump combined with a PV solar collector was developed using TRNSYS. The results showed that 55 % more electric energy was produced with the improved system, and that the electricity consumption was reduced by 23 % with 11 % less wasted heat [10].

Frost build-up is one of the challenges that heat pump technology faces during cold weather. There are two main methods for a defrost of the evaporator; reverse cycle of the refrigerant combined with an auxiliary element for back-up heating [11], and hot gas bypass method, where the refrigerant completely skips the condenser and expansion valve lines and directly flows from the compressor to the evaporator [12]. During the hot-gas bypass method, there is no heat output to the condenser, therefore the COP of the heat pump during defrost in this case would be zero. However, the advantage of this method is that there is no sudden peak in power demand. The compressor operates normally, and the hot refrigerant is warm enough to remove any frost build-up on the outdoor heat exchanger. As for the reverse cycle method, during the frost removal operation, the auxiliary element provides back-up heating to the condenser [11]. Depending on the power capacity of the heating strips, the COP of the heat pump during defrost mode could reach around 0.5. The reason for that is the heating strips are 100 % efficient and need electrical power as well, which could lead to sudden peak in power demand [11]. Usually, the defrost removal operation continues for a duration of 5 to 10 min. It is considered that 5 min time is enough in most cases to melt the deposited ice from the evaporator [13].

Vapour injection is said to help reducing the time for a defrost cycle. In an experiment involving an air source heat pump with vapour injection, the results showed a drop of almost 8 % in the duration of defrost cycle, and a defrosting efficiency increasing up to 54 % [15]. In

general, reverse cycle defrost operation is used to remove the frost accumulation on the outdoor unit of a heat pump. In traditional defrosting, the melted ice is flowing downwards. Research implementing a local drainage during defrost was made and compared to the traditional frost removal cycles. The results indicated that the energy consumption during a defrost cycle using a local drainage of the melted frost can drop by around 18 %, and that the defrosting efficiency can increase by roughly 10 % [16]. However, there are not many experiments done in relation to air source heat pumps with trans-critical carbon dioxide and the reverse cycle defrosting impact on the CO<sub>2</sub> trans-critical system. A study focused on proposing an optimized control strategy for the expansion valve opening and the frequency of the compressor suggested that with the optimized reverse cycle for frost removal this can reduce the defrost time by 95 s and decrease the energy consumption by almost 22 % [17]. There are different technologies within the heat exchangers that can affect the frost removal processes. In research studying the frosting behaviour and comparing microchannel and finned-tube heat exchangers indicated through experimental study that finned-tube heat exchangers can reduce the defrost time by almost 60 % and the energy consumption by about 55 % compared to micro-channel heat exchangers. The overall efficiency of the defrost operation of the finned-tube unit was almost 23 % higher [18].

Limited research has been found in literature regarding the effect of the defrost cycles of air source heat pumps and overall performance in different cold climates and the impact on their efficiency. More specifically, what would the power demand of the heat pump be in relation to the ambient temperature. Especially, the house insulation must be considered as it has a crucial role of how the air source heat pump would perform due to heat losses from various building elements (i.e., walls, windows, etc.). Each of these elements are built from different materials which have a specific thermal conductivity; hence, it can affect how fast a house can be warmed up, and how much are the heat losses. Also, not much research has been found to address frost build-up and defrost cycles effect on energy consumption, heat output, and the grid's peaks. There is still a need to study the effect of ambient temperatures on the number of defrosting operations on global level. References [7–10] have looked at how heat pumps affect the grid, and simulation work on that have been performed, but have not tested how the defrost cycle affects the performance and the power demand; Papers [15] and [16] have investigated the defrosting efficiency, and [17] and [18] explored the energy consumption during defrost operations, but none of them have involved how the ambient temperature affects the defrost cycles, and

they have not performed a simulation and mathematical analysis.

### 1.1. Climates and winter

The ambient temperature is dependent on the geographical location. For example, Polar climates in North Europe (e.g. Scandinavian countries) have very cold and long winters [19]. Lower temperatures usually lead to higher heat consumption, which will increase the electricity consumption of heat pumps. The lower the ambient temperature the higher the power demand of the heat pump in order to deliver the desired heat demand and with an increased possibility of defrost cycles in many cases. Fig. 1a presents the location of the 10 different cities covered in this study. It is evident that Helsinki, Harbin, and Moscow have considerably lower average winter temperatures compared to, for example, Nottingham. Fig. 1b presents the average, minimum and maximum temperatures for a typical metrological year (TMY) in winter months. For this paper, the weather data was acquired from PVGIS tool website [20].

### 1.2. Heat pumps

In recent years heat pumps have become a popular choice to provide heating and thermal comfort. A typical air source heat pump has a coefficient of performance (COP) of about 2.5, whereas a ground source heat pump's COP can reach 3.5–4 [21]. Air source heat pumps are a popular choice due to their lower price and ease of installation, however ground source units are more efficient, especially in cold weather. When the temperature drops below freezing, frost could accumulate on the outdoor unit of the air-source heat pump (ASHP) and causes drop in performance; hence a mode is triggered to remove the frost build-up, which increases the electricity consumption further if auxiliary element is used [22]. With hot-gas bypass method, this would lead to lower heat output affecting the dwelling demand. Defrost mode is something that owners do not have full control over. In most cases for a heat pump to trigger a frost removal cycle, there must be a certain pressure drop occurring in the evaporator section of the system and the ambient air temperature is below zero. Generally, each unit's pressure drop can vary, so the chances of every heat pump triggering a defrost cycle at the same time are low, but it is certainly not impossible [11]; particularly with possible overlaps. Another method for triggering defrosting operations is through time control [11]. As of 2019, there are approximately 238,823 installed units in the UK, 85 % of which are air



Fig. 1a. Map of the world with the investigated cities.

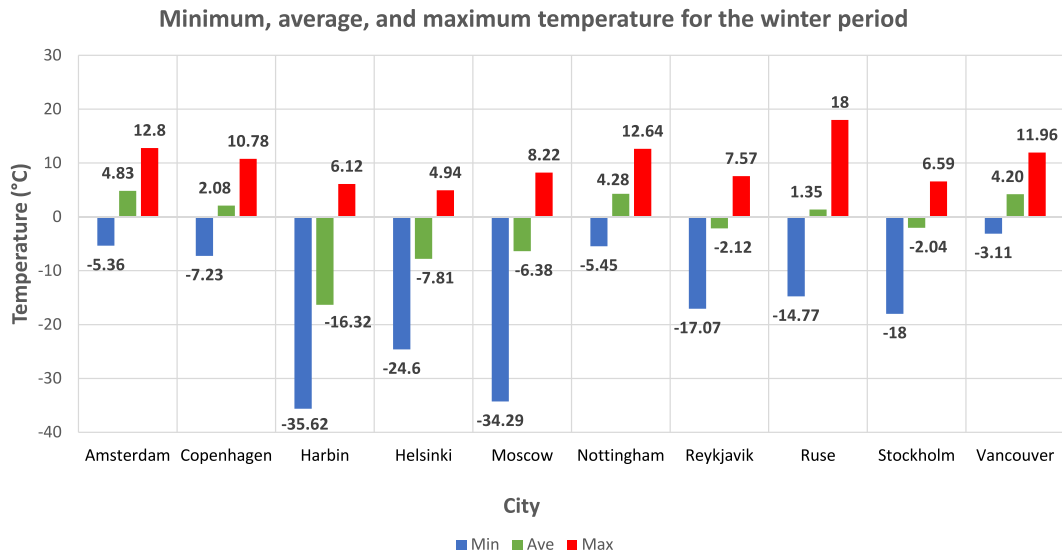


Fig. 1b. Average winter temperatures in different cities, based on data from [19].

source heat pumps [23]. Nevertheless, limited research has been done in the effect of the defrost cycle of air source heat pumps on the grid, and the impact of the ambient temperature on the power demand of the device. This paper will address some of the limitations in the current state-of-the-art to inform future technology development and strategies.

## 2. Methodology

Fig. 2 represents the methodology used for this research. A novel software simulating an air source heat pump is designed and developed to assess the electricity consumption and heat output. This includes modules related to efficiency of the heat pump, defrost cycles and building insulation model. The model has been validated experimentally using a specially designed test-rig. In total 10 different global cities are chosen, and weather data is applied to simulate heat pump power demand with defrost cycles. Analysis of the number of defrost cycles is presented for each city. This has been applied for 3 months winter period of cold weather. The coldest days in the winter season for each city are

chosen to evaluate the effect of defrost cycles on the power demand and heat output of an air source heat pump. Based on the results, the expected effect on the electricity demand due to the heat pumps and their defrost cycles is presented. After that, a novel heat pump power demands vs ambient temperature look-up chart based on the local climate and housing insulation was developed for the 10 cities. This allows researchers to use the model to simulate the grid demand in any of the 10 cities using the proposed simulation model. The UK grid is selected for the detailed presentation of results to show how the model and the lookup chart could be implemented to assess the overall effect on the electricity grid and energy consumption using the suggested methodology.

## 3. The heat pump simulation model and the defrost cycles

In order to estimate the energy consumption and heat output by the heat pump, and calculate the energy needed for the defrost cycle, it was necessary to acquire the appropriate data. Fig. 3 presents a schematic

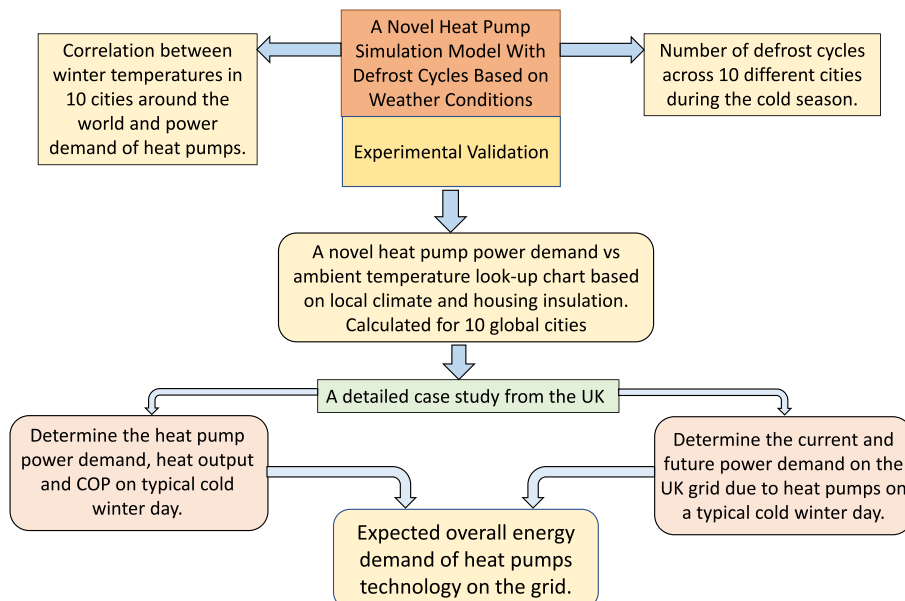


Fig. 2. The suggested methodology flowchart.

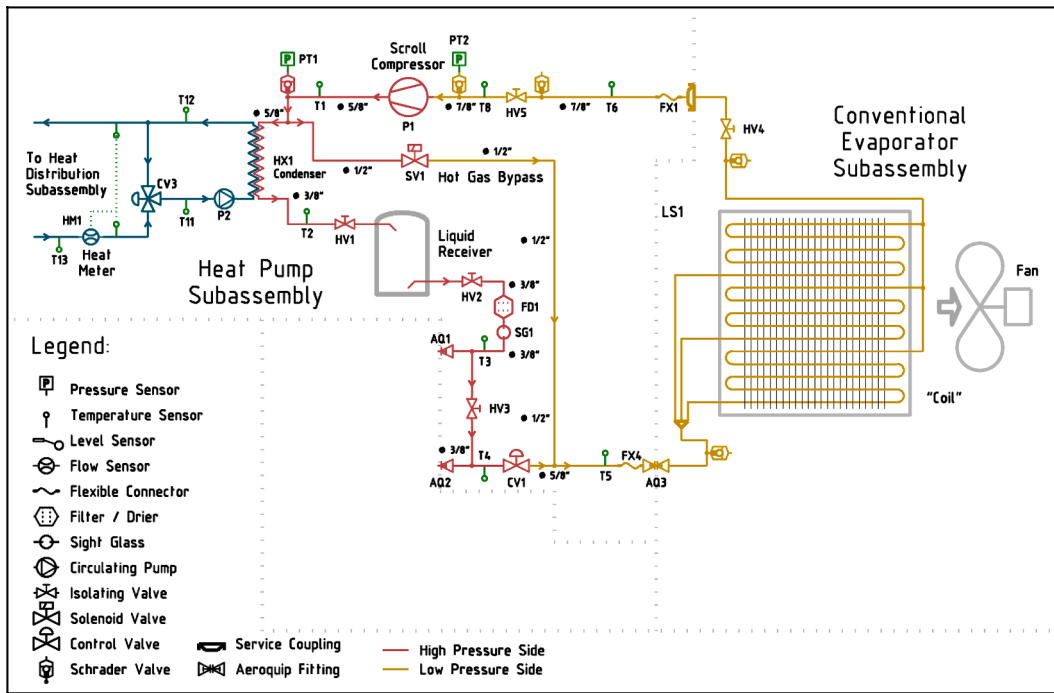


Fig. 3. A schematic diagram of the test rig of the air source heat pump.

diagram of the air source heat pump test rig that has been experimentally validated and simulated; it shows how the components are connected. Fig. 4 presents the heat pump test rig with the evaporator/fan assembly. A software simulation of the air source heat pump via Simulink/MATLAB has also been built, see Fig. 5. Fig. 5 presents the detailed Simulink block diagram of the modules to simulate the heat pump technology and estimate the need for the defrosting cycles; and the following sub-sections present the mathematical equations of the simulation.

Prior to the Simulink model, a test rig of the air source heat pump is designed and used to conduct the needed experimental work at cold winter temperatures to see how the system performs under cold climate conditions. The test was conducted for 180 min, and a defrost cycle was triggered at the final 10 min of the experimental work. The reasoning for the specific timings is to see if the performance of the heat pump would be affected by the accumulating frost on the outdoor heat exchanger when run for a prolonged period of time without frost removal operations. The conducted experimental work with the test rig is designed to validate the simulation model. A simulation process is conducted afterwards using the same conditions. The data that has been captured from both the experimental and simulation work included compressor power rate (kW), heating power (kW), total energy consumption (kWh),

total heating delivered (kWh). The melted frost from the test rig's evaporator is collected after the defrost cycle in a vessel and the quantity is measured. This determined how much frost (L) is accumulated during the experiment. The parameters are then compared with that of the simulation for further validation of the modelled frost build-up processes.

The swept volume of the compressor chosen for the simulation is a ZH21 K4E PFJ-524 scroll compressor with a swept volume of 8.04 m<sup>3</sup>/h. The condenser is a plate heat exchanger capable of delivering space and water heating, and the evaporator is a finned tube coil heat exchanger (model DX SA 33T 2R 12FPI 860L 11N), combined with aluminium fins for an increased heat transfer area. The area of the evaporator is 0.7151 m<sup>2</sup>. Dimensions of the evaporator are 850x842x150mm. In addition, for the defrost mode, we chose the hot gas bypass as it would be sufficient to remove ice build-up on the outdoor heat exchanger without excess increase of power demand by the heat pump method. For the simulation, the heat pump power demand and the maximum heat output were considered. In the simulation, a typical weather data was used from the 10 considered global cities. The simulation provided information on when defrost mode was triggered and the power demand by the unit. Fig. 5 presents the detailed Simulink block diagram of the modules to simulate the heat pump technology and estimate the need for the

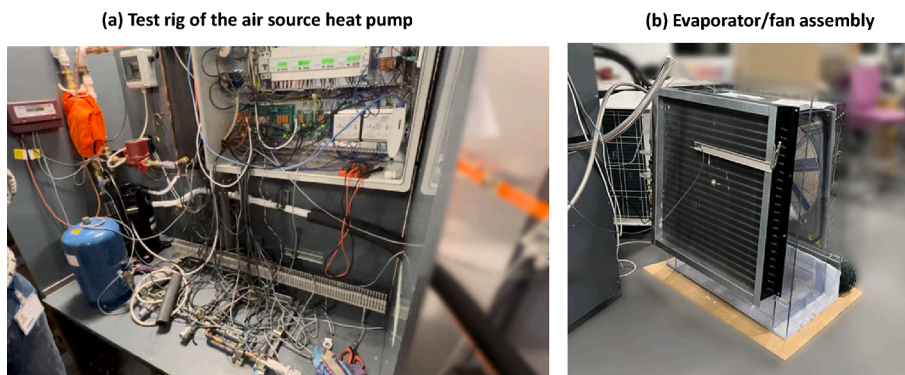


Fig. 4. The test rig of the air source heat pump and the evaporator/fan assembly.

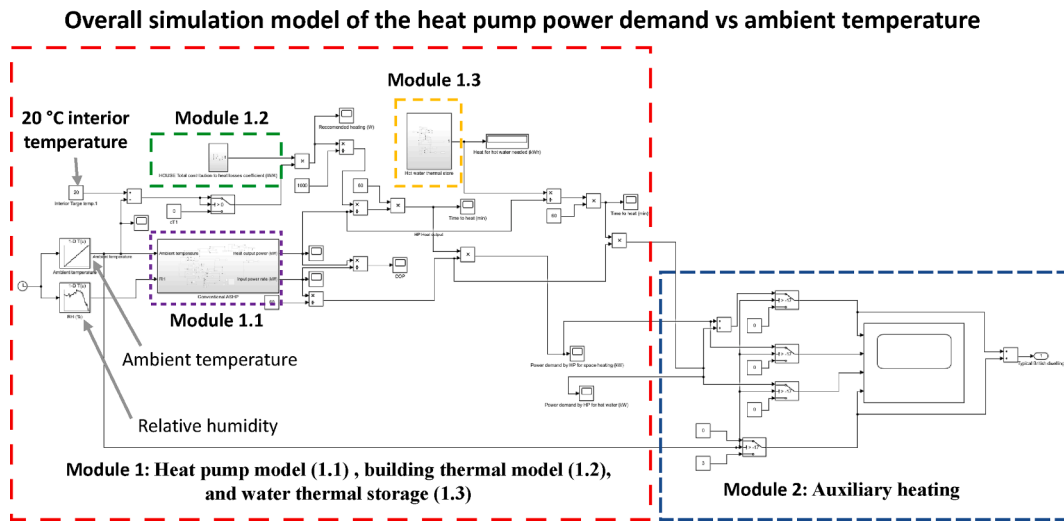


Fig. 5. Main modules of the heat pump demand vs ambient temperature.

defrosting cycles; and the following sub-sections present the mathematical equations of the simulation.

The simulation was first conducted for a period of three months in the cold season between 1st December and 28th February as the temperature in the northern hemisphere tends to drop considerably during that time [19]; and using an assumed scenario in which the heat pump was working constantly providing both space and water heating. When the real temperature dropped below 0 °C the defrost mode was triggered 80–90 min later and the frost removal operation ran for approximately 5 min. It is estimated that it is possible for air source heat pumps to function for 80 to 90 min while frost has accumulated on the outdoor heat exchanger [13]. It is also estimated that in most cases 5 to 10 min is enough to run the defrost cycle and remove the ice build-up [14]. When the ice was removed from the outdoor unit, the normal refrigeration cycle continued.

The weather data look-up table in Simulink required the simulation time to be interpolated due to the segments of input data. The weather data was acquired from PVGIS tool website [20]. The website provides data for a typical meteorological year. The data that was acquired from

the tool was ambient temperature and relative humidity for the 10 cities that are included in this research. The extrapolated values are then fed to the heat pump simulation. This allows the simulation to determine the heating capacity of the evaporator and the condenser, as well as the input power rate of the compressor. A target temperature for the inlet of the condenser was set to 50 °C. The relative humidity data was required as it affects the frost growth rate on the outdoor heat exchanger. The simulation model was divided into different sub-modules, which are described in more details in the following sections.

3.1. Module 1: Heat pump model, building thermal model, and water thermal storage

In Module 1, the models of the air source heat pump, the contribution to heat losses of the house/building elements, and the water thermal storage were constructed. Fig. 4 presents further details regarding Module 1. Fig. 6 shows the model configuration of the air source heat pump, the contribution to heat losses from the building elements which include floor, roof, windows, and walls, and the model of the hot water

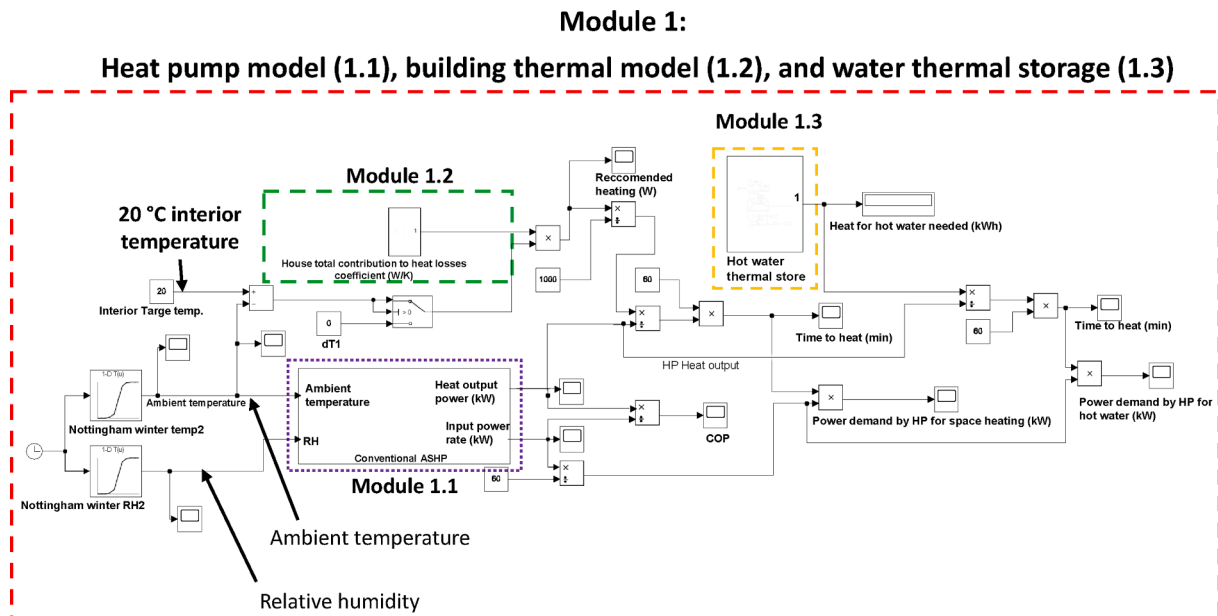


Fig. 6. Module 1 of the simulation model.

thermal storage as well. Each of the sub-modules are described into more details in the following sections.

3.1.1. Module 1.1: Air source heat pump model

Fig. 7 presents the configuration of the heat pump along with the frost growth rate, compressor’s power input rate, evaporation and condenser power. The main parameters that were monitored were power consumption, heat output and coefficient of performance (COP).

In the Mass flow rate sub-module, the mass flow rate of the system is calculated. This parameter is determined by the compressor’s swept volume, which is given by the manufacturer and the specific volume, which the model is designed to extrapolate using the R134a refrigerant’s enthalpy – pressure (P-h) diagram.

Where the swept volume of the compressor for one second  $V_{Sw1}$  can be expressed using the following equation [24]:

$$V_{Sw1} = V_{Sw} \cdot \tilde{A} \cdot 3600 \tag{1}$$

where  $V_{Sw}$  is the swept volume of the compressor ( $m^3/h$ );  $V_{Sw1}$  is the swept volume of the compressor representing the value per second ( $m^3/s$ ) [24].

The mass flow rate can be expressed as:

$$\dot{m} = V_{Sw1} \cdot \tilde{A} \cdot V_{sp} \tag{2}$$

where  $\dot{m}$  is the mass flow rate of the refrigerant (kg/s);  $V_{sp}$  is the specific volume of the refrigerant, which is extrapolated by a look-up table from the pressure – enthalpy diagram of R134a, the refrigerant that was used in the simulation and experimentally. All the required processes within the vapour – compression cycle are considered by the model [25].

In Module 2 the heat capacity of the evaporator is calculated. This is done using a developed 2-D look-up table of the P-h diagram in Simulink. The model extrapolates the appropriate enthalpy values and multiplies them by the mass flow rate.

a) Evaporation and compression sub-module

The evaporator heat capacity can be expressed as:

$$Q_{ev} = \dot{Q} \times (h_2 - h_1) \tag{3}$$

where  $Q_{ev}$  is the evaporator heat capacity (kW);  $h_2$  is the enthalpy at the outlet and  $h_1$  is the enthalpy at the inlet of the evaporator (kJ/kg), extrapolated by a look-up table using the pressure enthalpy diagram of R134a [25].

The compressor power rating can be calculated as:

$$P_{com} = \dot{m} \times (h_3 - h_2) \tag{4}$$

where:  $P_{com}$  is the compressor power rating (kW);  $h_3$  is the enthalpy at the outlet of the compressor (kJ/kg), extrapolated from the pressure – enthalpy diagram considering all the vapour-compression processes involved [24,25].

There we first had to determine the compressor’s efficiency. After the refrigerant reaches the target temperature of 50 °C it then passes through the condenser in the evaporation and compression sub-module where the heating capacity is calculated by first determining the enthalpy difference at that stage and multiplying it by the mass flow rate. It is expected the temperature at the condenser inlet to vary slightly due to the interaction of many components with the refrigerant.

b) Condensation sub-module – Condenser heating capacity

The condenser heating capacity can be calculated as:

$$Q_c = \dot{m} \times (h_3 - h_4) \tag{5}$$

where  $Q_c$  is the condenser heating capacity (kW);  $h_4$  is the enthalpy at the condenser outlet (kJ/kg) extrapolated from the R134a chart considering the occurring processes of the vapour – compression cycle [24,25].

c) Frost growth rate sub-module

In this sub-module the most novel sub-system where the frost build-up on the outdoor unit (evaporator) simulation is conducted. A novel numerical model was developed which predicts the frost layer on the outdoor heat exchanger. In order to evaluate the novel numerical model,

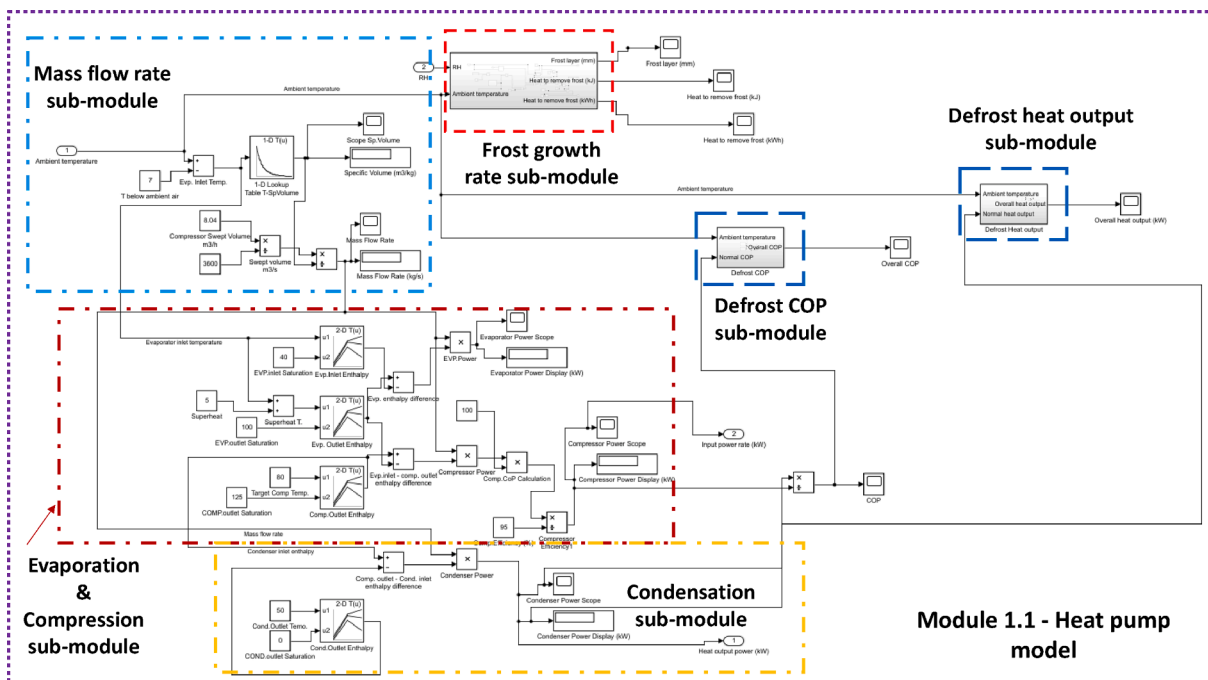


Fig. 7. The suggested air source heat pump model (Module 1.1).

it was compared with already existing methods.

The equation for the existing frost build-up model can be expressed as:

$$\delta_{ice} = 0.12 \times [t \times (T_a - T_s)]^{0.43} \quad (6)$$

[26]; where  $\delta_{ice}$  is the frost layer thickness (mm);  $t$  is the time from which the frost starts accumulating (s),  $T_a$  is the ambient temperature (K);  $T_s$  is the heat exchanger surface temperature (K); 0.12 is a constant.

Due to the high thermal conductivity of the coils, the coil surface and refrigerant temperature are assumed to be at the same temperature.

The above equation does not include the relative humidity which has a crucial role on the frost growth rate; as the higher the humidity and the lower the temperature the more frost build up will occur. Therefore, this paper has included the relative humidity as discussed in the methodology and this has been validated experimentally as will be seen in the following sections. The implemented novel numerical model can be expressed as:

$$\delta_{ice} = \frac{\{(V_{hx} \times S_a) \times t\} \times \rho_{air}}{A_{evp}} \times HR \quad (7)$$

Where:  $V_{hx}$  is the volume of the outdoor heat exchanger ( $m^3$ );  $S_a$  is the evaporator air velocity (m/s) which is provided by the manufacturers;  $t$  is the time from which the ice starts building up (s);  $\rho_{air}$  is the air density ( $kg/m^3$ );  $HR$  is the humidity ratio (kg/kg) which is extrapolated from psychrometric charts;  $A_{evp}$  is the area of the outdoor heat exchanger ( $m^2$ ). A simulation of 24 h was conducted for both frost growth rate models, see Figs. 8 and 9. Fig. 8 shows graphically the relative humidity and the ambient temperature during the comparison of both frost build-up modes comparison. The data was taken from PVGIS [20] from Ruse, Bulgaria, as the city can get very cold and humid during the winter period.

Fig. 9 presents graphically the frost layer thickness from both numerical models. The standard model does not take into consideration the relative humidity and the heat exchanger size, and that is why it shows a constant value of 7.8 mm. With the novel suggested numerical model, the humidity and size of the outdoor heat exchanger are taken into consideration and the results are more dynamic and change according to the temperature and relative humidity. Each drop of the graph represents a defrost cycle taking place. In both cases, the heat pump was working for approximately 80 min before a 5 min defrost operation occurred. The simulation shows that the depth of frost layer is much less than the standard method but at the same frequency. This would mean a faster defrosting process.

Fig. 10 presents how the frost growth rate was implemented in Simulink. The sub-module also includes a counter of defrost cycles. There is a switch block which uses the ambient temperature as a threshold, if it drops below 0 °C, ice starts forming on the evaporator. The frost layer thickness is monitored. From there the model calculates

Novel vs standard frost growth rate numerical model

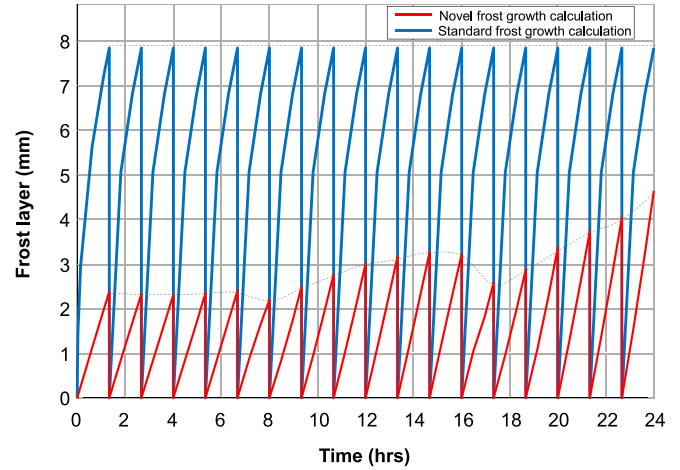


Fig. 9. Novel vs standard frost growth rate numerical model.

the energy needed to remove the frost build-up. The mass of the ice layer accumulated is calculated as:

$$m_{ice} = V_{ice} \times \rho_{ice} \quad (8)$$

where  $m_{ice}$  is the mass of the ice layer accumulated on the outdoor unit (kg);  $V_{ice}$  is the volume of the ice layer ( $m^3$ );  $\rho_{ice}$  is the density of the ice layer ( $kg/m^3$ ).

The heat needed to remove the ice build-up can be expressed as:

$$Q_{removelce} = m_{ice} \times 333.55 \quad (9)$$

where  $Q_{removelce}$  is the heat needed to remove the ice build-up on the outdoor unit (kJ); 333.55 is the heat fusion of ice (kJ/kg).

The heat needed to remove the ice deposition on the outdoor unit is expressed as:

$$Q_{ice-rem} = Q_{removelce} \div 3600 \quad (10)$$

where  $Q_{ice-rem}$  is the heat needed to remove the ice deposition on the outdoor unit (kWh);  $Q_{removelce}$  was divided by 3600 to convert from kJ to kWh.

d) Defrost COP sub-module

In this sub-module, the System performance is calculated by dividing the heating capacity by the compressor's power rating.

$$COP = Q_c \div P_{com} \quad (11)$$

Relative humidity and ambient temperature

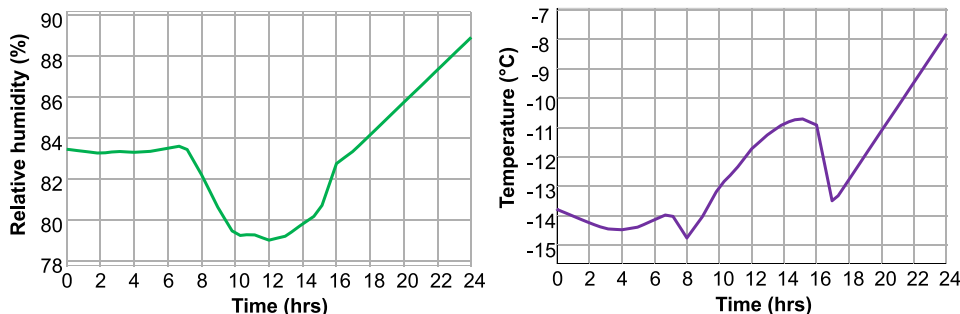


Fig. 8. Relative humidity and ambient temperature that are used to simulate and compare the frost growth rate models.

Frost growth rate module

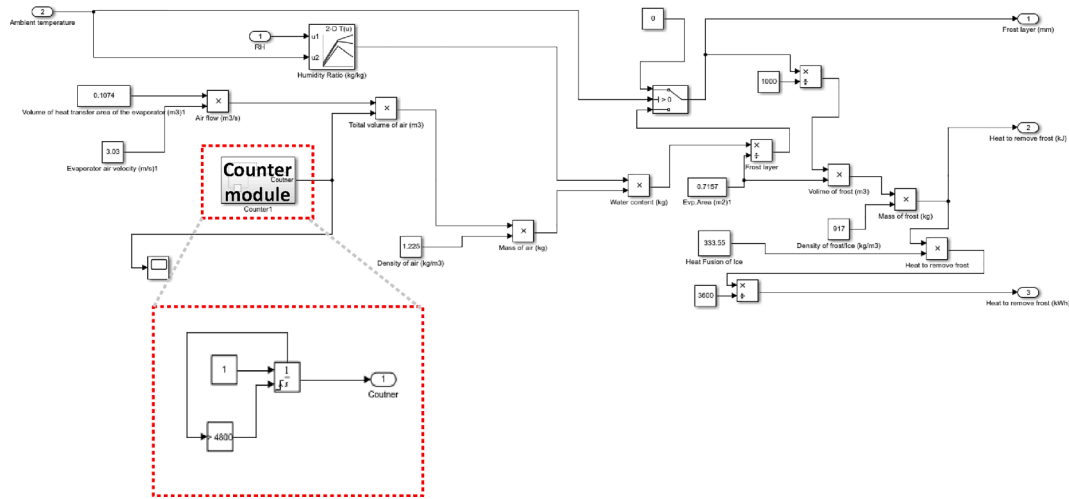


Fig. 10. Frost growth rate sub-module.

where COP is the coefficient of performance. The sub-module also includes the COP during defrost. When the hot gas bypass method is used the COP is 0 as no heat is delivered to the condenser. Instead, the refrigerant goes from the compressor directly to the outdoor heat exchanger.

e) Defrost heat output sub-module

This sub-module monitors the heat output by the condenser, and it also takes into account the defrost cycles of the system where no heat is delivered.

Fig. 11 shows how the defrost heat output sub-module was built in Simulink. Two counters were also included whose role is to consider the time when defrost cycles take place. The defrost COP model was built in the same way, but in the place of (2), normal heat output, the system COP was connected to the 2nd switch block. It is assumed that the defrost cycle is triggered before a the frost layer causes any significant heat transfer degradation, which was validated experimentally.

3.1.2. Module 1.2 - building energy simulation

In order to simulate the energy demand needed for a heat pump in a household, there will be a need to simulate the dynamic performance of the house itself where the heat pump is used; as the demand for heating

will depend on the level of insulation and the dimensions/architype of the house. In this paper, a detailed model of energy building insulation and heating demand was analysed for a typical average house for each of the 10 cities. The same methodology can be conducted for any other city or country as suitable. In this section, a model of a house in each of the 10 countries is created in Simulink, see Fig. 12. The aim of this model is to showcase the losses of heat in the dwelling and the daily heating demand which is also driven by the ambient temperature. This to allow the accurate simulation of the heating demand required by the heat pump. Fig. 12 presents the contribution to heat losses coefficient from the house elements, which include windows, floor, roof, and walls. The purpose of this paper is to use average house size and thermal specifications to predict the heating demand for each country. A more accurate simulation can be achieved normally with further specific house design at well-defined location and orientation. In our case, the purpose was to provide a reasonable estimation for heating demand. Solar heating was not included, particularly that defrosting cycles in most cases would happen at night and with the absence of solar radiation.

Numerically this can be expressed as [27]:

$$C_{hlc} = (0.33 \times ACH \times V_h) + \{(A_1 \times U_1) + (A_n \times U_n) \dots\} \tag{12}$$

where  $C_{hlc}$  is the total contribution to heat losses coefficient (W); 0.33 is a constant;  $ACH$  is the air changes per hour in the house;  $V_h$  is the volume of the house ( $m^3$ );  $A_1$  is the area of an building element of the house ( $m^2$ );  $U_1$  is the U-value of an building element of the house ( $W/m^2 K$ ).

Module 1.2 determines the space heating demand of the house and further estimates the power demand by the heat pump. Table 1 provides information about the dwelling size and heat transfer coefficient from the building elements such as windows, walls, roof, and floor. That information has been acquired through policies and energy efficiency requirements depending on the country, see Table 1.

The values from Table 1 are used to conduct the simulation for the heat pump power demand for a duration of 3 months during the winter season. In addition, a look-up chart was developed using Simulink and Table 1 data to provide an approximate estimation of the air source heat pump expected demand depending on the ambient temperature.

The power demand by the heat pump can be expressed as:

$$P_{sh} = \left[ \left( \frac{(C_{hlc} \times \Delta T) \cdot \tilde{A} \cdot 1000}{Q_{HPout}} \right) \times 60 \right] \times P_{comp} \tag{13}$$

where  $P_{sh}$  is the power demand by the heat pump for space heating (kW);

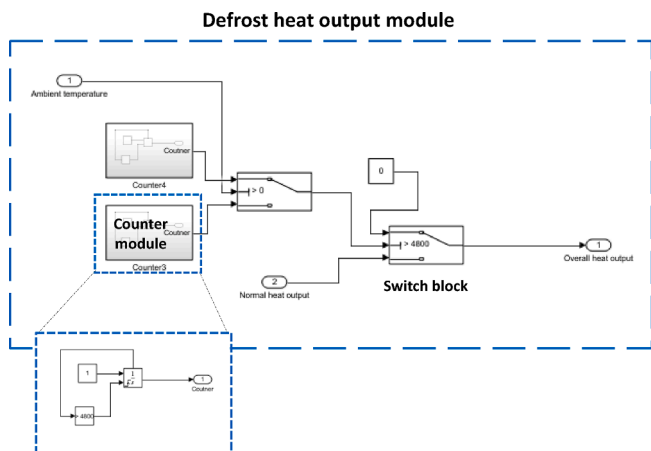


Fig. 11. Defrost heat output sub-module in Simulink.

**Module 1.2: Contribution to heat losses coefficient from building elements**

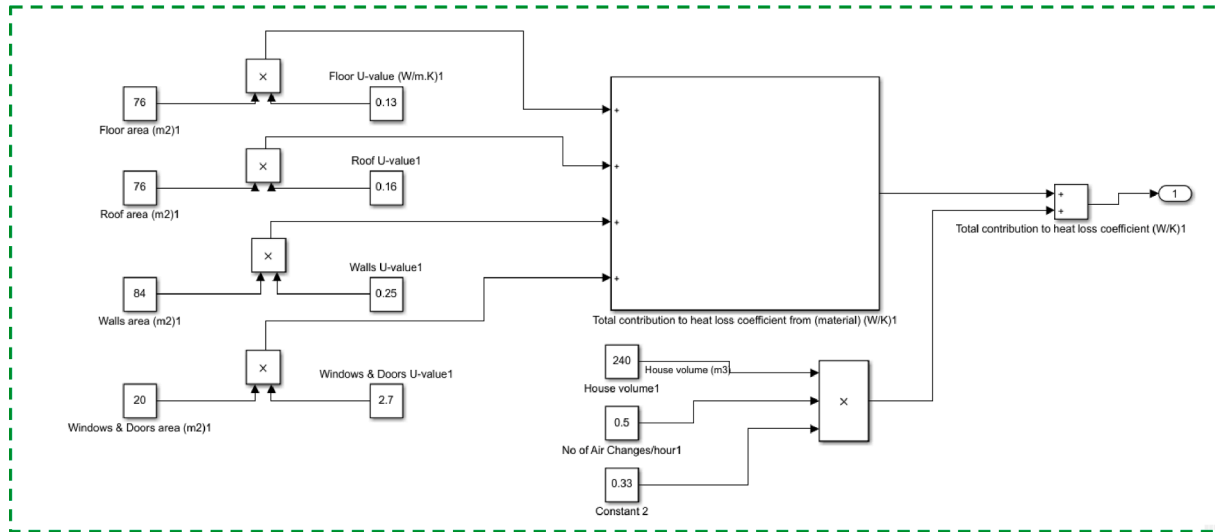


Fig. 12. Modules of the building heat transfer simulation model.

**Table 1**  
Typical characteristics of building elements of dwellings in each country.

Country	A <sub>house</sub>	U <sub>walls</sub>	U <sub>floor</sub>	U <sub>roof</sub>	U <sub>window</sub>	ACH	A <sub>wall</sub>	A <sub>window</sub>	V <sub>house</sub>	References
Bulgaria	67.6	0.28	0.28	0.28	0.7	0.23	82	19	170	[28]
Canada	177	0.21	0.14	0.14	1.6	0.6	122	27	407	[29,30,31,32]
China	60	3.8	4	3.5	2.5	0.25	84	5.25	162	[33,34]
Denmark	98.8	0.3	0.2	0.2	1.8	0.23	99	15	247	[35,36]
Finland	75.8	0.17	0.16	0.09	1	0.2	87	8	189	[35,36]
Iceland	119	0.25	0.2	0.15	1.7	0.23	109	12	296	[35,36]
Netherlands	116	0.29	0.29	0.25	1.65	0.24	112	23	301	[36,39]
Russia	67	2.4	2.9	3.4	1.2	0.23	82	5.25	168	[38]
Sweden	90	1	1	1	1	0.22	95	20	225	[33,35]
UK	76	0.25	0.13	0.16	2.7	0.33	84	20	240	[37,40]

$Q_{HPout}$  is the heat output capacity by the heat pump (kW);  $P_{comp}$  is the compressor power rating (kW);

This part of the simulation not only determines the time needed to provide the required space heating but also the power demand by the heat pump to satisfy the heating demand.

Eq. (13) can also be used to estimate the power demand by the heat pump for hot water demand. In this case instead of  $C_{hcl}$  (the total contribution to heat losses coefficient), the hot water thermal storage capacity value must be used, which is determined by Eqs. (12) and (13), and module 1.3 in the simulation model, as described in the next section.

**3.1.3. Module 1.3 – Thermal storage**

Fig. 13 presents how Module 1.3 was built in Simulink. The role of the module is to monitor the hot water demand by the household and was further included in the total power demand by the heat pump.

The required heat for the hot water can be expressed as:

$$Q_{hw} = (V_{ts} \times \rho_w) \times Cp_w \times \Delta T \tag{14}$$

where:  $Q_{hw}$  is the heat needed for the hot water in the thermal storage (kWh);  $V_{ts}$  is the volume of the thermal storage,  $\rho_w$  is the density of water ( $kg/m^3$ );  $Cp_w$  is the specific heat of water ( $kJ/kg.K$ );  $\Delta T$  is the temperature difference between the hot water tank and the interior of the house (K).

The recommended heat for the hot water tank can be expressed as:

$$Q_r = (A_{ts} \times U_{ts}) \times \Delta T \tag{15}$$

where:  $Q_r$  is the recommended hot water tank thermal capacity (kW);  $A_{ts}$

**Module 1.3: Thermal storage**

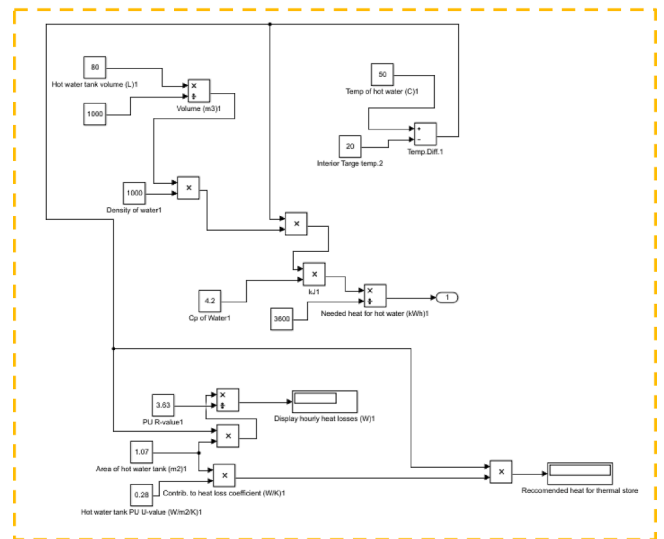


Fig. 13. Module 1.3, thermal storage model in Simulink.

is the area of the thermal storage ( $m^2$ );  $U_{ts}$  is the U-value of the thermal storage, which is comprised mostly of polyurethane filling acting as an insulation ( $0.28 W/m^2 K$ ).

### 3.2. Module 2

Module 2 in the simulation model is built through a series of switch blocks which monitor the ambient temperature, and when it reaches  $-17\text{ }^{\circ}\text{C}$  the heat pump switches off and a back-up electrical resistant heater with a capacity of 3 kW switches on. It has been estimated that at an ambient temperature of around  $-17$  and  $-20\text{ }^{\circ}\text{C}$  air source heat pumps tend to suffer and do not operate properly [41].

Fig. 14 shows how module 2 of the simulation model was built. When the ambient temperature drops below  $-17\text{ }^{\circ}\text{C}$ , a back-up electrical resistant heater switches on and provides the thermal energy needed to satisfy the demand for space heating and hot water. Note that a typical restarting temperature is  $-12.2\text{ }^{\circ}\text{C}$  for the residential heat pump; so that the difference between  $-17\text{ }^{\circ}\text{C}$  and  $-12.2\text{ }^{\circ}\text{C}$  creates the needed hysteresis to efficiently control the heat pump; and reduce wear and tear. However, for this paper it has been assumed in the simulation that the control system does not include hysteresis and assumed ideal control process for this purpose at  $-12.2\text{ }^{\circ}\text{C}$ .

## 4. Results

In this section, the validation of the simulation results is performed experimentally using the test-rig. In addition, the Simulink simulation of the heat pump for 10 international cities during the winter season are presented and discussed.

### 4.1. Simulink model validation

The heat pump test rig was operational for 170 min and the final 10 min were dedicated for a defrost cycle. The melted frost was collected, and its volume (L) measured. The temperature and humidity data can be seen in Fig. 15. Fig. 15 presents the temperature and humidity of variation throughout the validation experiment.

Fig. 16 represents the validation of the simulation model using the test rig data. Operating under the same conditions, the results from the Simulink model are almost the same as the test rig with small variations due to the complexity and variation and interaction of the actual components and interdependency.

Fig. 17 represents the total energy consumption and the total heat output comparison. The percentage errors of both parameter comparison are roughly 0.63 and 5.2 % respectively.

Fig. 18 presents the water content after the defrost cycle for both the test rig and the simulation. The results are very close with a percentage error of approximately 1.6 %.

The validation proves that the equations and assumptions that were used as foundation of the simulation model are reasonable, and that the Simulink model of the air source heat pump operates as expected with

very little variation.

### 4.2. Seasonal simulation in global cities

An analysis was done in order to determine the number of defrost cycles of an air source heat pump in various cities across the world. Fig. 19 presents the simulation results of the 3-months winter season for the 10 Cities. It is evident from Fig. 19 that the ambient temperature impacts the heat pump power demand. If the temperature drops low  $-17\text{ }^{\circ}\text{C}$  the back-up heating switches on, such as the case of Helsinki. Fig. 20 presents a summary of the number of defrost cycles for the 10 global cities. If we chose to take Helsinki or Harbin as an example, you will notice significant number of defrost cycles.

It is evident from Fig. 20, that the colder a region is, the more defrost cycles a heat pump will be going through. The winter in Helsinki and Harbin is considerably colder compared to Vancouver or Amsterdam. It is likely that more heat pump units can go through a frost removal operation at the same time, or overlap in the defrost cycle, which could cause a significant and sudden load on the grid.

Fig. 21 indicates that there is a strong relationship between the number of defrost cycles of heat pumps and the ambient temperature, with correlation coefficient of  $-0.94$ . The lower the ambient temperature, the more frost removal operations are done by heat pump.

### 4.3. Temperature vs average power demand

A novel look-up chart has been generated, see Fig. 22, to present the power demand for an average household across the 10 selected cities in kW for each different ambient temperature between  $-20\text{ }^{\circ}\text{C}$  and  $+20\text{ }^{\circ}\text{C}$  for air source heat pump and resistive electric heaters. For example, the power required for the heat pump as shown in Fig. 22 is reduced with the increase in temperature above  $0\text{ }^{\circ}\text{C}$  and increases at negative temperatures due to the defrost cycles and reduction in efficiency. However, at very low temperatures ( $-17\text{ }^{\circ}\text{C}$ ) the heat pump becomes ineffective for heating and hence the system switches to resistive heating. Fig. 22 is very important graph as it presents, for each city dwelling, the expected power demand for heat pumps. This will support the analyses of the effect of that collectively on the grid, which will be discussed in the next sections taking the UK grid as an implementation case study.

The results from Fig. 22 also consider the size of the average dwelling in each city and the U-values of the building elements such as windows, walls, roof, and floor. This graph can be used as a look-up table for each of the analysed cities for an approximate prediction of the air source heat pump power demand for space and hot water heating depending on the ambient temperature, assuming a typical average insulation level of a buildings as in Table 1. Fig. 19 is also evidence of the importance of better insulation of dwellings. Fig. 22 presents a novel generic graph that

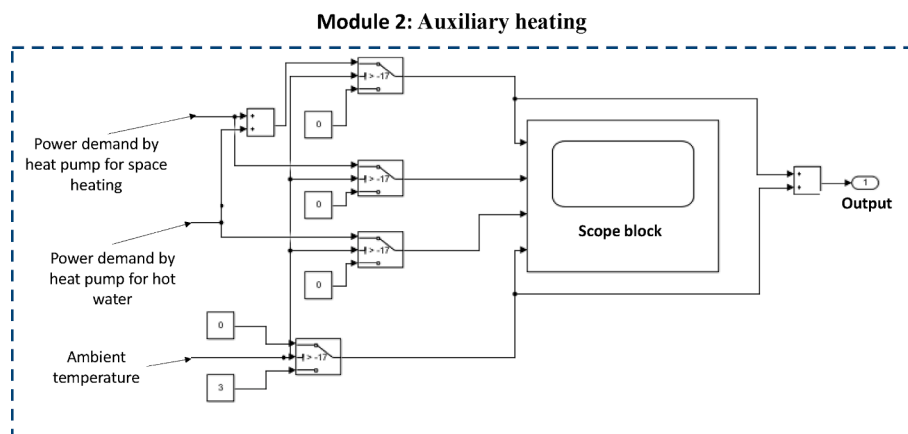


Fig. 14. Module 2 of the simulation model.

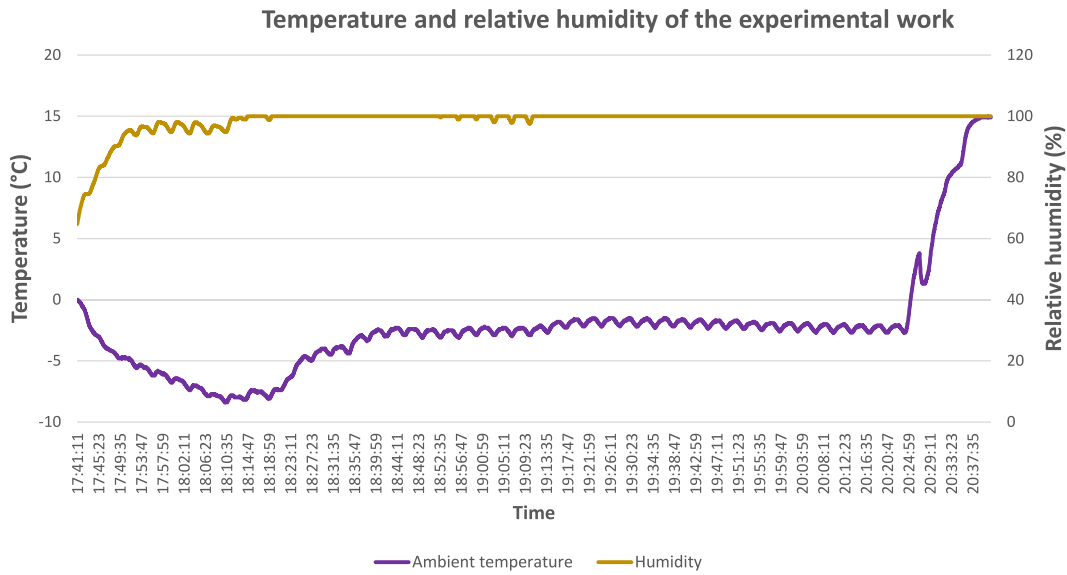


Fig. 15. Temperature and relative humidity of the test rig experimental work.

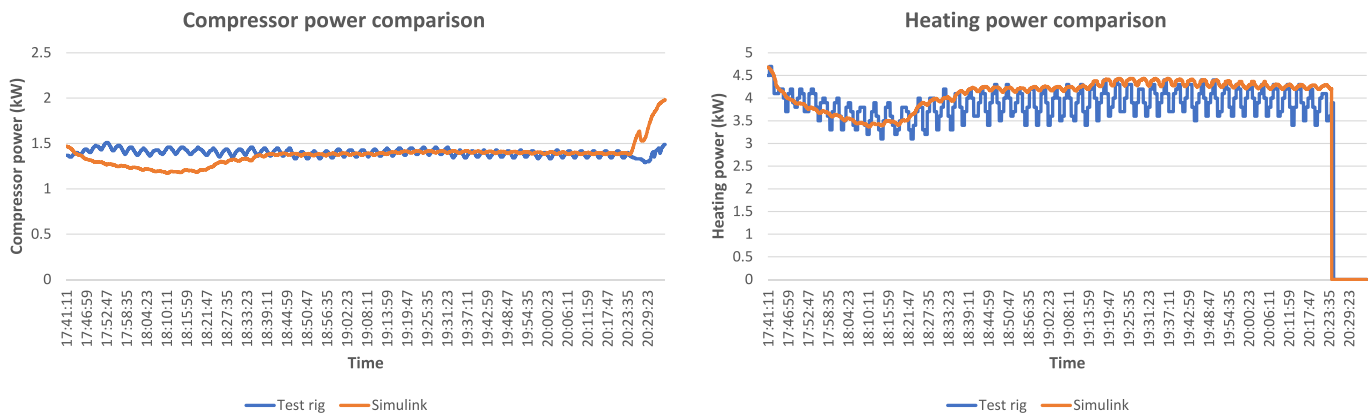


Fig. 16. Compressor power and heating power comparison.

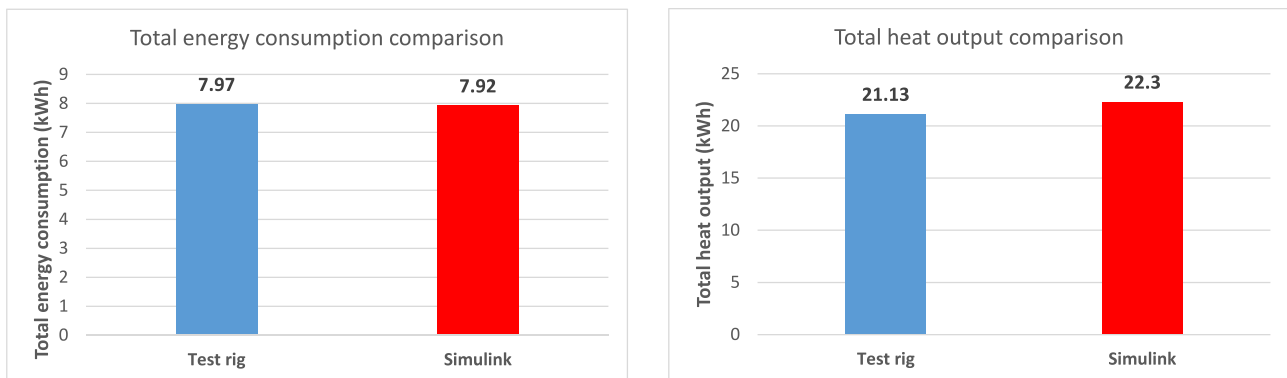


Fig. 17. Total energy consumption and total heat output comparison.

outlines a typical household power demand at different temperatures for a heat pump to provide the required heating at specific location and a typical insulation levels as specified in Table 1. An assumed 3kW backup resistive electric heater is expected to operate for temperatures below  $-17^{\circ}\text{C}$  to provide some heating which may or may not be sufficient to provide the required heating demand. For example, the backup electric heater will be sufficient for well insulated residential houses at ow

temperatures; but will not be sufficient for poorly insulated houses. In countries, such as Finland and Bulgaria which tend to have better insulation of the building elements would have lower heat pump power demand compared to places such as the Russia and China where insulation of the buildings tend to be insufficient leading to increased power demand.

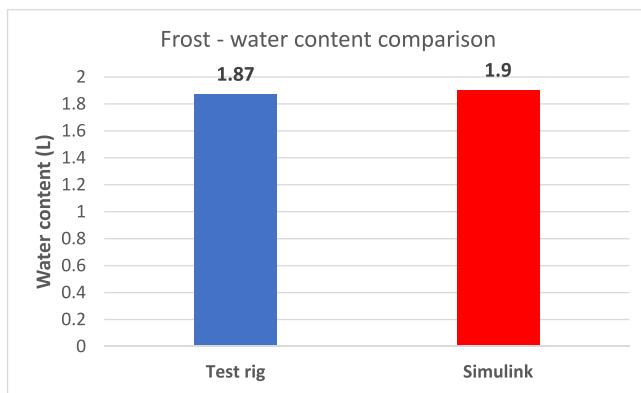


Fig. 18. Frost/water content comparison.

#### 4.4. Heat pump and their defrost cycles and the effect on the UK grid

Based on the above results, equations and Fig. 22, UK electricity grid is discussed in detail as an implementation case study. This is in order to provide more detailed analysis of how the electricity consumption by heat pumps and their defrost cycles would influence the electricity grid. For simplicity, the UK has been selected for the detailed case study while the approach can be generalised in any country or city. To start with the analysis of the demand curve, it was necessary to determine the daily electricity consumption of a typical cold day, see Fig. 23 [42]. The grid load was monitored on a typical cold day where the ambient temperature was between  $-1$  to  $-3$  °C [20].

The Gridwatch [42] allowed the data collection of the hourly numerical values for the electrical consumption and the identification of the type of source that generated the energy, including international connections to other grids. Currently, the grid mix consists of the following sources of electrical energy production [42]: Gas (40.6 %), Wind and solar (23.8 %), Nuclear (17.3 %), Coal (2.1 %), Oil and other fusels (2.8 %), hydro (1.8 %) and other renewables (11.5 %). Around 40 % of the electricity is generated via combined cycle gas turbines. In the past recent years (2018–2020), the capacity of wind and solar has increased considerably [43], whereas the capacity of coal-fired power stations was reduced. In recent years, the UK has reduced its dependency on fossil fuel considerably and shifted its focus to more eco-friendly solutions to produce the required electricity. In this section, the effect of heat pumps is presented. Since Nottingham is located in the Midlands, an assumption is made to consider its weather conditions as an average for the UK as a whole. The daily power demand during the cold season in the UK for a duration of three months is considered and discussed.

Fig. 24 presents graphically the heat output and the COP, and power demand by the heat pump on a typical cold day in Nottingham, UK. In addition to these graphs, charts for the ambient temperature, relative humidity, and frost layer thickness on the outdoor heat exchanger are also provided. The power demand corresponds to the heating demand for the dwelling, and it takes into account the U-values of the building elements. It can be noted that the frost build-up layer is affected by the humidity in the air. The higher the humidity content, the thicker the frost layer on the heat exchanger. The drops of heat output and COP represent the defrost cycles. Each time a frost removal operation occurred, the heat output and therefore the performance dropped to 0 as no heat was delivered to the condenser.

Based on the number of households in the UK (27.8 million), Fig. 25 shows a comparison between the current electricity consumption and the assumed consumption with heat pump units installed in every household in the UK under the same conditions. Such loads can cause disturbance to the grid. The daily electricity consumption increases to approximately 144 % assuming every household adopts heat pump technology which is always in operation.

Peaks in electricity demand are more common during winter,

especially during times when more of the population are trying to heat their homes and heat water. Fig. 25 shows that between 7:00–11:00 and 17:00–19:00 there is a peak in demand due to heating need when people arrive from work. This suggests that power stations in the UK need to increase their power capacity to satisfy the demand.

Fig. 26 below presents the current electricity demand in the cold winter season in the UK. With the help of the novel heat pump Simulink model, we have determined what would be the situation if all 27.8 million households in the UK operate air source heat pumps with overlapping times.

Fig. 26 presents the comparison between the current and the expected electricity demand if every household in the UK is equipped with a heat pump. The average daily energy consumption would increase by roughly 106 % over the whole winter period.

## 5. Discussion

In recent years, the electricity demand in the UK has decreased; household energy usage has dropped due to milder winters in the last 6 years [43]. Since 2012 the energy consumption of households in the UK has dropped from 115 TWh to 105 TWh [44]. Electricity generation has also decreased too since 2012 from around 325 TWh per annum to approximately 307 TWh in 2019 [45]. As the country has plans to electrify the transportation, this could lead to further increase in power demand in the future. As such it was estimated that for the UK this would lead to approximately 86.3 TWh or 22 % increase in demand, including the grid losses [46,47].

Fig. 27 compares the current supply of electricity from power stations with the expected energy demand on the grid from the heat pumps. The overall load when combining all 27.8 million heat pumps in such a scenario, would increase by approximately 144 % on a typical cold day in the UK.

This paper has explored the scenario of fully electrified heating and examined the impact this has on the grid. Even though it is highly unlikely that all heat pump systems would go through a defrost cycle at the same time, the electricity network must be prepared in case there is sudden demand on the grid due to the defrost cycle in extreme cold weather conditions. Furthermore, some dwelling may own other types of heat pumps, such as ground source. However, as air source ones are more popular due to their lower price and ease of installation, some of them may be equipped with auxiliary elements putting more stress on the electrical grid. That is why in most cases it may be advisable to owners to defrost via hot-gas bypass method as it would not affect the grid as much. In addition, the ambient temperature in the UK rarely drops below freezing whereas in Scandinavian countries this is more common due to the regular cold winter seasons. In this research, several assumptions are made including the scenario of every UK household owning an air-source heat pump; this probably will not be the case as there are currently 250,000 units installed of which approximately 213,000 are air-source units. The reason more people choose this type of installation is because the initial investment cost is lower than the ground-source variants. If this trend is maintained this would suggest that around 85 % of households will own air-source heat pumps. Furthermore, there are options to improve the performance of the heat pumps and their impact on the grid. A research aiming to provide constant power supply to a heat pump in order to reduce the grid fluctuations, managed to achieve that by combining the heating device with a hot water thermal storage [48]. This not only reduced the peak times by approximately 60 per cent, but also it showed to reduce the bills by around 22 per cent [48]. Thermal storage can play important role for the efficiency of heat pump systems. In a study conducted in two primary schools in China, found out that in normal winter scenario, there is an excessive thermal energy delivered by the heat pump due to inefficient control strategy [48]. In order to improve that, the study conducted a simulation of the heat pump combined with heat storage. The results from that research showed that almost 51 per cent of total thermal

### Temperature of the 10 cities and the related power demand of heat pumps

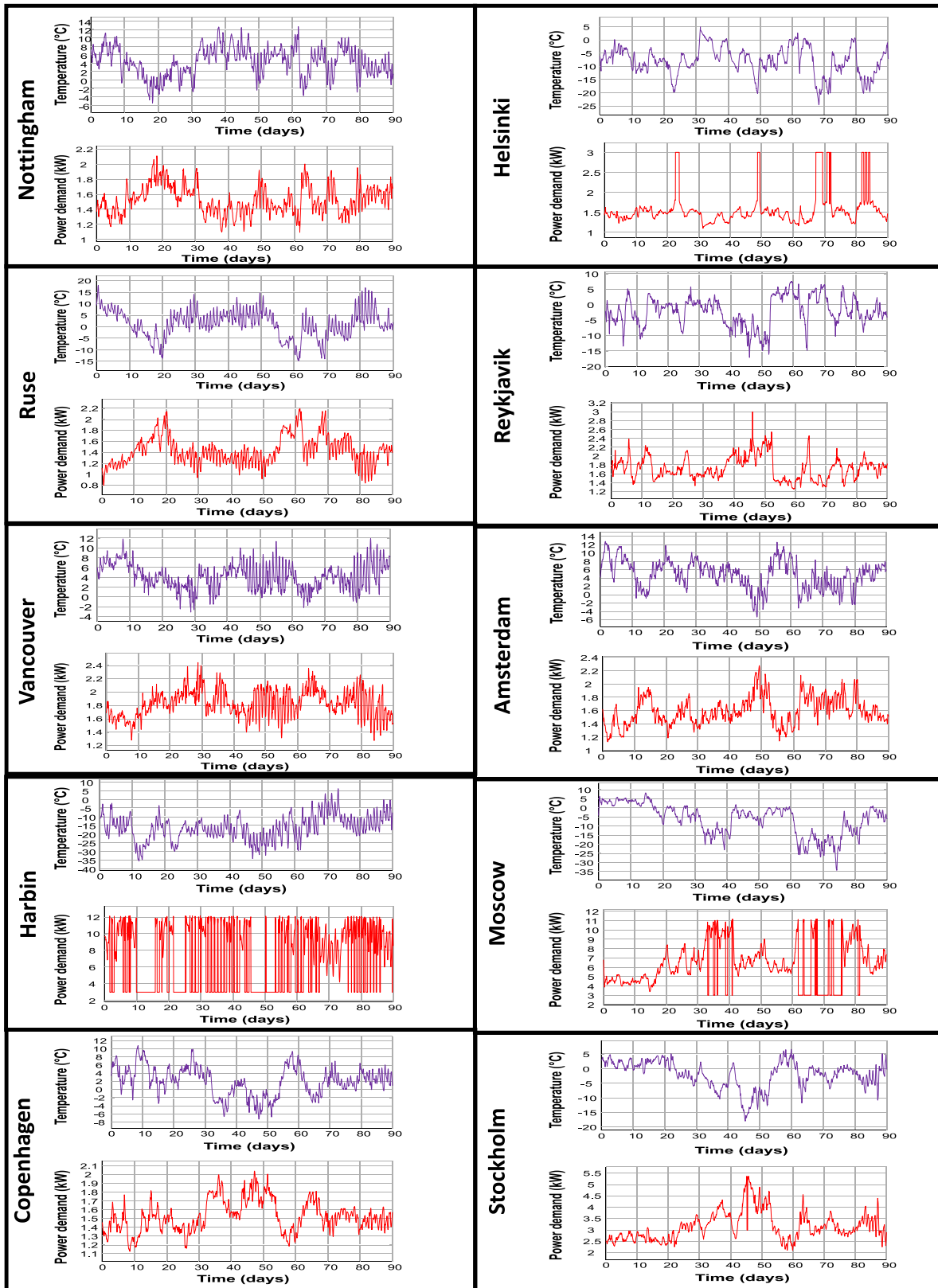


Fig. 19. Temperature of the 10 cities and the related performance of the heat pump.

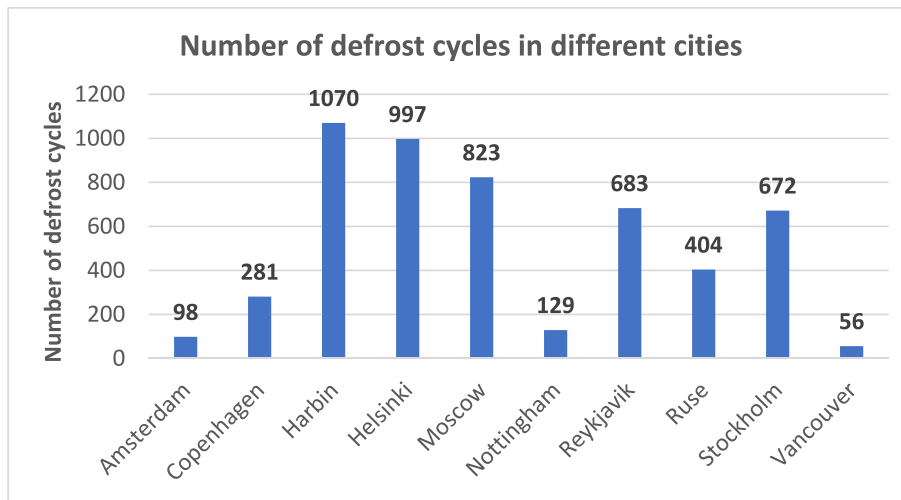


Fig. 20. Number of defrost cycles in various cities during the cold season.

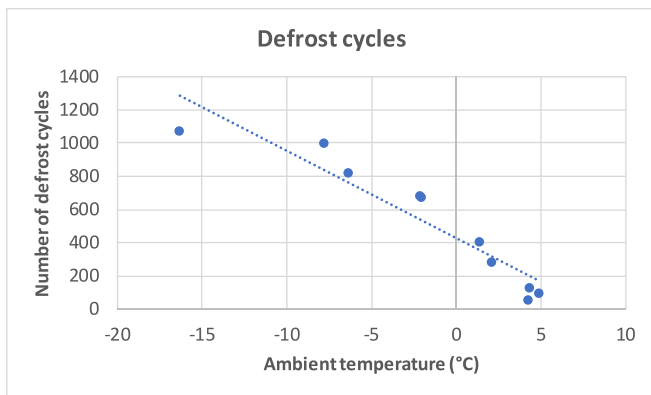


Fig. 21. Correlation between number of defrost cycles and ambient temperature.

energy consumption can be saved using heat storage [49].

It must be noted that climate can play a crucial role on the performance of air source heat pump as this study suggests. Furthermore, a

research assessing weather air source heat pumps can provide reliable thermal energy to mild, cold, and very cold climate areas in Canada, concluded that air source heat pump systems would have lower efficiency in colder climates in the country (i.e. Toronto, Quebec) [50]. In addition, because of the higher power demand, this could lead to increased greenhouse gas emissions [50].

Furthermore, the U-values and dwelling size provided by the policies and insulation might not be an accurate reflection of the whole building stock. In most cases the insulation type and thickness is controlled by the house owners, hence these values can vary from one dwelling to another.

One of the other assumptions is that we have assumed that the industrial, commercial sector and public transportation sectors' demand will stay the same in terms of electricity demand and the focus was on domestic households.

In the simulation conducted, it was assumed a conventional system would be able to provide up to 95 kWh of heating per day and have a compressor with a swept volume of around 8 m<sup>3</sup>/h. Each household would probably acquire a higher capacity heat pump unit or a lower one depending on their demand. In addition, heat pump owners could apply for the renewable energy incentive scheme which provides financial

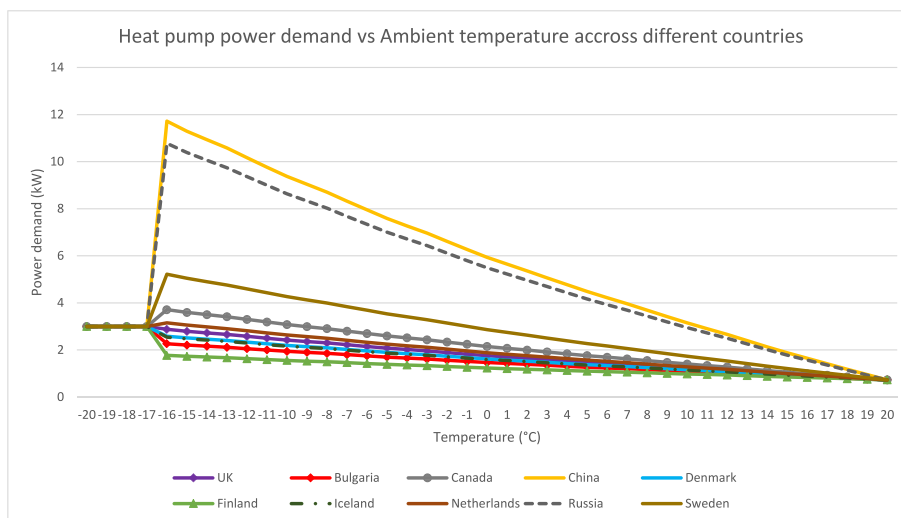


Fig. 22. A novel generic graph that presents a typical household power demand at different temperatures for a heat pump to provide the required heating at specific location and a typical insulation levels (see Table 1) (an assumed 3 kW backup resistive electric heater is expected to operate for temperatures below -17 °C to provide some heating which may or may not be sufficient to provide the required heating demand).

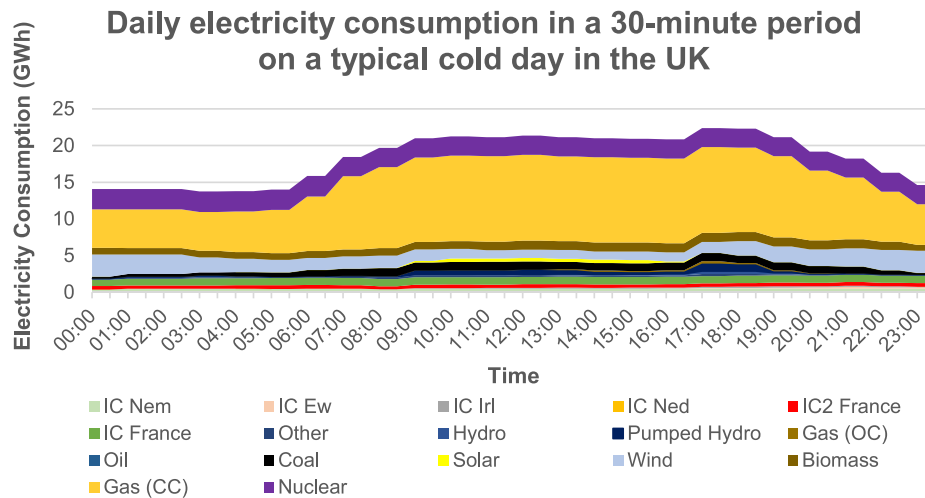


Fig. 23. A typical current daily winter electricity consumption in a 30-minute period in the UK (based on data from Gridwatch [42]).

## Heat output, COP, and power demand by the heat pump on a typical cold day in Nottingham

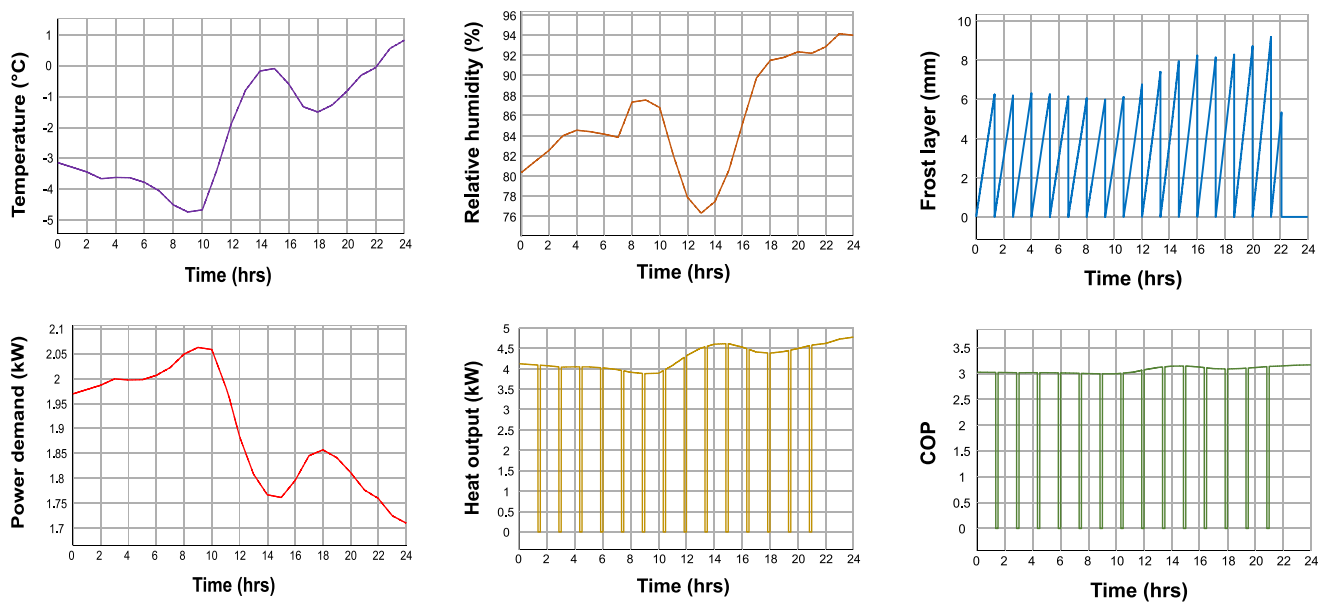


Fig. 24. Heat output, COP, and power demand by the heat pump in Nottingham.

support per kWh of electricity/heating provided by such systems [51] in case of the UK. On global level, governments should consider gradual support to renewable energy for a better management of the grid and have a better control on grid demand. Taking into consideration the climate in the UK, it is highly unlikely the demand of energy would suddenly increase dramatically as the temperature will not likely plummet below freezing, hence defrost cycles will rarely be required by heat pumps.

Another important point to consider is the sources of electricity, as this will affect the carbon emission levels in the UK when the transport and heating sectors are electrified. It is expected by 2050 that the UK would have completely reduced its reliance and utilisation of fossil fuels, which includes power stations. The key question to consider here is what electricity generation mix is going to be used. If more wind turbines, solar panels, and nuclear power stations are used for the main power production, then the final CO<sub>2</sub> emissions would be lower than expected,

as these three sources provide the cleanest electricity as their carbon intensity is below 100 gCO<sub>2</sub>eq/kWh.

### 6. Conclusion

This paper has investigated a scenario whereby heating is assumed to be fully electrified for the domestic residential sector, using air source heat pumps. The paper has discussed the defrosting cycles of air source heat pumps based on the weather in 10 global cities and the possible effect this could have on the electricity grid. The research also shows that there is a relationship between ambient temperature and the number of defrost cycles a heat pump unit will go through. A novel graph that links the expected power demand for heating with the change in temperature is introduced. The research also investigates the importance of better insulation in dwellings. The load on the electricity grid can be expected to increase in the future in most countries due to the

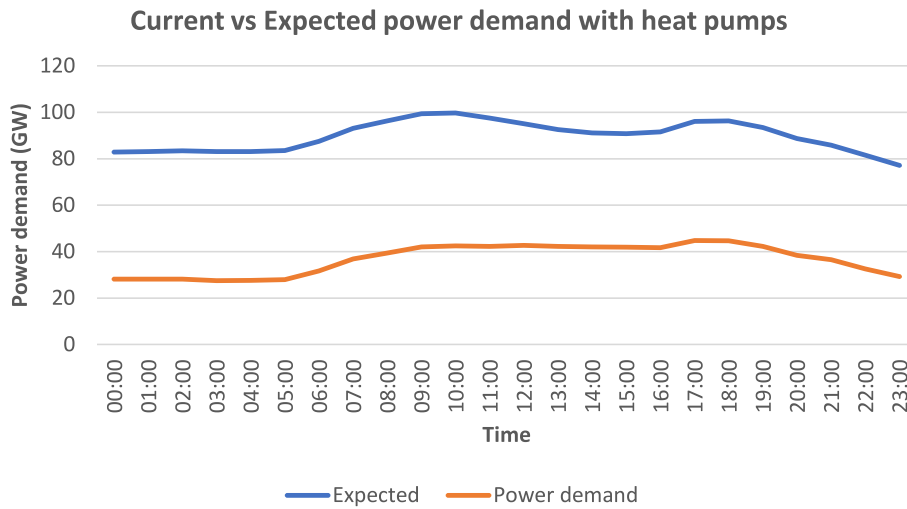


Fig. 25. Analysis of one day energy demand comparison in the UK with current demand and the heat pumps.

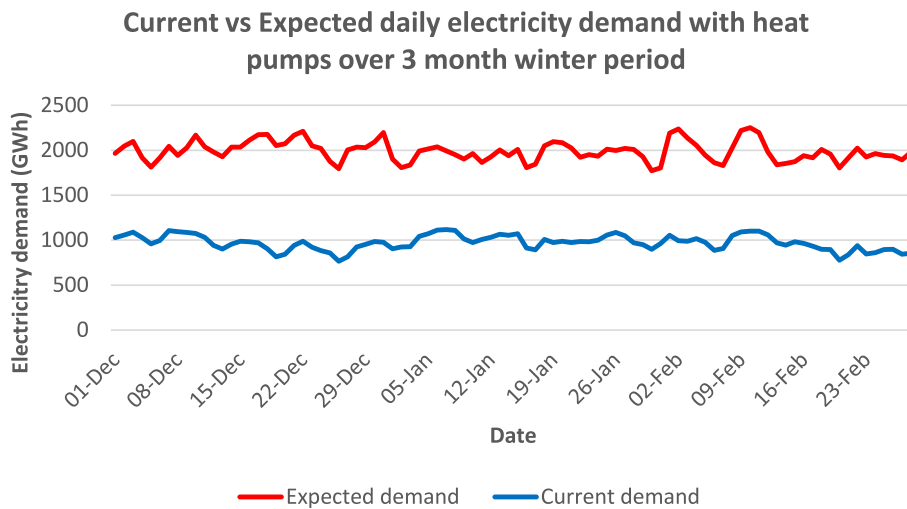


Fig. 26. The electricity demand comparison for the period between 1st December – 28th February between current use and expected demands using heat pumps.

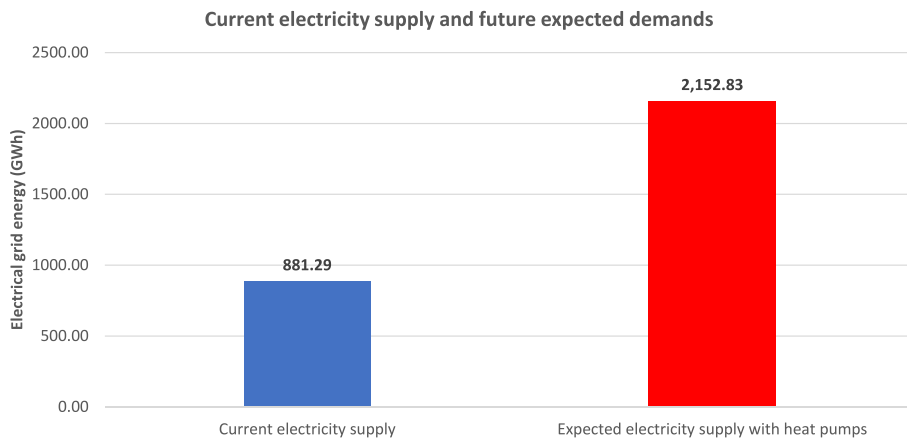


Fig. 27. A comparison between the current and expected electric grid energy demand (UK-daily in winter).

drive to net zero Carbon emission and reduction of fossil fuel use for heating applications. This power demand is expected to increase in cold weather due to poor housing insulation in certain locations.

The novelty of this paper is that it provides prediction of the

frequency of the defrost cycles in any city based on the created look-up chart (Fig. 22) of temperature vs power demand of heat pumps to estimate power demand. This has been done via a novel Simulink model to develop a heat pump simulation that includes defrost cycles and

buildings heating demand. An experimental validation was also implemented to validate and ensure the accuracy of the simulation model. A comprehensive implementation case study of the UK grid is presented; which can be used as a research method for different locations in the world to predict the power demand and heat output by heat pumps including during defrost cycles.

### Declaration of Competing Interest

The authors declare that they have no known competing financial interests or personal relationships that could have appeared to influence the work reported in this paper.

### Data availability

Data will be made available on request.

### Acknowledgments

The authors would like to thank DTA3 COFUND H2020/Marie Skłodowska-Curie PhD Fellowship programme for partially funding this research work (Grant Agreement Number: 801604).

### References

- [1] S. Dong, E. Kremers, M. Bruccoli, R. Rothman, S. Brown, Techno-enviro-economic assessment of household and community energy storage in the UK, *Energ. Convers. Manage.* 205 (2020), 112330.
- [2] BBC News, 2021. Petrol and diesel car sales ban brought forward to 2035. [online] Available at: <<https://www.bbc.co.uk/news/science-environment-51366123>> [Accessed 20 April 2021].
- [3] Carbon Brief. 2021. Analysis: UK is now halfway to meeting its 'net-zero emissions' target | Carbon Brief. [online] Available at: <[https://www.carbonbrief.org/an-alyis-uk-is-now-halfway-to-meeting-its-net-zero-emissions-target#:~:text=\(Net%2Dzero%20is%20formulated%20in,below%201990%20levels%20by%202050.&text=UK%20territorial%20greenhouse%20gas%20emissions,net%2Dzero%20target%20for%202050.\)](https://www.carbonbrief.org/an-alyis-uk-is-now-halfway-to-meeting-its-net-zero-emissions-target#:~:text=(Net%2Dzero%20is%20formulated%20in,below%201990%20levels%20by%202050.&text=UK%20territorial%20greenhouse%20gas%20emissions,net%2Dzero%20target%20for%202050.))> [Accessed 20 April 2021].
- [4] Climate Change Committee, 2021. Reaching Net Zero in the UK - Climate Change Committee. [online] Available at: <<https://www.theccc.org.uk/action-on-climate-change/reaching-net-zero-in-the-uk/>> [Accessed 20 April 2021].
- [5] IEA. 2021. Achieving net-zero emissions by 2050 – World Energy Outlook 2020 – Analysis – IEA. [online] Available at: <<https://www.iea.org/reports/world-energy-outlook-2020/achieving-net-zero-emissions-by-2050>> [Accessed 20 April 2021].
- [6] G. Koreneff, M. Ruska, J. Kiviluoma, J. Shemeikka, B. Lemström, R. Alanen, T. Koljonen, Future development trends in electricity demand, *VTT Tied – Valt. Tek. Tutkimusk* (2009) 1–84.
- [7] S. Bae, Y. Nam, Comparison between experiment and simulation for the development of a Tri-generation system using photovoltaic-thermal and ground source heat pump, *Energ. Buildings* 231 (2021), 110623.
- [8] B. Xiang, Y. Ji, Y. Yuan, D. Wu, C. Zeng, J. Zhou, 10-year simulation of photovoltaic-thermal road assisted ground source heat pump system for accommodation building heating in expressway service area, *Sol. Energy* 215 (2021) 459–472.
- [9] M. Dannemand, I. Sifnaios, Z. Tian, S. Furbo, Simulation and optimization of a hybrid unglazed solar photovoltaic-thermal collector and heat pump system with two storage tanks, *Energ. Convers. Manage.* 206 (2020), 112429.
- [10] D. Wu, H. Yan, B. Hu, R. Wang, Modeling and simulation on a water vapor high temperature heat pump system, *Energy* 168 (2019) 1063–1072.
- [11] B. Langley, *Heat Pump Technology*, 3rd ed., Pearson, 2001, pp. 1–440.
- [12] D. Huang, Q. Li, X. Yuan, Comparison between hot-gas bypass defrosting and reverse-cycle defrosting methods on an air-to-water heat pump, *Appl. Energy* 86 (9) (2009) 1697–1703.
- [13] Y. Chung, S.-I. Na, J.W. Yoo, M.S. Kim, A determination method of defrosting start time with frost accumulation amount tracking in air source heat pump systems, *Appl. Therm. Eng.* 184 (2021), 116405, <https://doi.org/10.1016/j.applthermaleng.2020.116405>.
- [14] V. Payne, D.L. O'Neal, Defrost cycle performance for an air-source heat pump with a scroll and a reciprocating compressor, *Int. J. Refrig* 18 (2) (1995) 107–112, [https://doi.org/10.1016/0140-7007\(95\)93893-o](https://doi.org/10.1016/0140-7007(95)93893-o).
- [15] W. Wei, L. Ni, W. Wang, Y. Yao, Experimental and theoretical investigation on defrosting characteristics of a multi-split air source heat pump with vapor injection, *Energ. Buildings* 217 (2020), 109938.
- [16] M. Song, G. Xie, L. Pekař, N. Mao, M. Qu, A modeling study on the reverse cycle defrosting of an air source heat pump with the melted frost downwards flowing away and local drainage, *Energ. Buildings* 226 (2020), 110257.
- [17] Y. Wang, Z. Ye, Y. Song, X. Yin, F. Cao, Experimental analysis of reverse cycle defrosting and control strategy optimization for transcritical carbon dioxide heat pump water heater, *Appl. Therm. Eng.* 183 (2021), 116213.
- [18] T. Xiong, Y. Ying, B. Han, G. Yan, J. Yu, Comparison of energy supplies and consumptions in heat pump systems using finned tube and microchannel heat exchangers during defrosting, *Int. J. Refrig.* (2021).
- [19] Geography.learnontheinternet.co.uk. 2021. Internet Geography. [online] Available at: <<http://www.geography.learnontheinternet.co.uk/topics/climatezones.html>> [Accessed 6 September 2021].
- [20] European Commission, 2021. JRC Photovoltaic Geographical Information System (PVGIS) – European Commission. [online] Available at: [https://re.jrc.ec.europa.eu/pvg\\_tools/en/#PVP](https://re.jrc.ec.europa.eu/pvg_tools/en/#PVP) [Accessed 2 June 2021].
- [21] Evergreen Energy, 2016. Heat Pump Efficiency: How Efficient are Heat Pumps? - Evergreen Energy. [online] Available at: <<https://www.evergreenenergy.co.uk/he-at-pumps/how-efficient-are-heat-pumps/>> [Accessed 21 April 2021].
- [22] The Renewable Energy Hub. 2020. Heat pumps - Functioning of heat pumps | The Renewable Energy Hub. [online] Available at: <<https://www.renewableenergyhub.co.uk/main/heat-pumps-information/how-do-heat-pumps-work-in-cold-weather/#:~:text=Why%20Air%20Source%20Heat%20Pumps%20Lose%20Efficiency%20in%20Cold%20Weather&text=The%20air%20source%20heat%20pump%20is%20typically%20sized%20to%20be,heating%20requirements%20for%20your%20home>> [Accessed 21 April 2021].
- [23] de Best, R., 2021. UK: number of heat pumps in operation 2019 | Statista. [online] Statista. Available at: <<https://www.statista.com/statistics/740491/heat-pumps-in-operation-uk/>> [Accessed 21 April 2021].
- [24] P. Byrne, R. Ghoubali, J. Miriel, Scroll compressor modelling for heat pumps using hydrocarbons as refrigerants, *Int. J. Refrig* 41 (2014) 1–13.
- [25] Evans, P. (2019) R134a pressure enthalpy chart, *The Engineering Mindset*. Available at: <https://theengineeringmindset.com/r134a-pressure-enthalpy-chart/> (Accessed: December 1, 2022).
- [26] S. Mengjie, et al., Frost layer thickness measurement and calculation: A short review, *Energy Procedia* 142 (2017) 3812–3819.
- [27] The Open University, n.d. Energy in Buildings - Calculating Heat Losses. [online] Open Learn. Available at: <<https://www.open.edu/openlearn/nature-environment/energy-buildings/content-section-2.4.1>> [Accessed 6 January 2022].
- [28] Republic of Bulgaria Ministry Of Energy, 2017. National Long-Term Programme For The Promotion Of Investments In Measures Aimed At Improving The Energy Performance Of The National Stock Of Public And Private Residential And Commercial Buildings 2016–2020.
- [29] International House Sizes (no date) Demographia. Available at: <http://demographia.com/db-intlhouse.htm> (Accessed: December 2, 2022).
- [30] Building Code requirements, 2019. Ontario. Available at: <https://www.ontario.ca/document/build-or-buy-tiny-home/building-code-requirements> (Accessed: December 2, 2022).
- [31] Canadian Energy Codes Status (2018) Fenestration & Glazing Industry Alliance. Available at: <https://fgiaonline.org/news/canadian-energy-codes-status> (Accessed: December 2, 2022).
- [32] The Ontario Building Code | Minimum Window Areas (no date) BuildingCode. Online. Available at: <https://www.buildingcode.ontario.ca/1293.html> (Accessed: December 2, 2022).
- [33] J. Li, B. Shui, A comprehensive analysis of building energy efficiency policies in China: Status quo and development perspective, *J. Clean. Prod.* 90 (2015) 326–344. Available at: 10.1016/j.jclepro.2014.11.061.
- [34] D. Lai, et al., Window-opening behavior in Chinese residential buildings across different climate zones, *Build. Environ.* 142 (2018) 234–243. Available at: 10.1016/j.buildenv.2018.06.030.
- [35] Sand, H., Lorenzen, K.H. and Nittegaard, C.B., 2012. Survey of green legislation and standards in the construction area in the Nordic countries.
- [36] Average size of dwelling by household type and degree of urbanisation (no date) Knoema. Knoema. Available at: <https://public.knoema.com/hhpzpre/average-size-of-dwelling-by-household-type-and-degree-of-urbanisation?regionID=IS> (Accessed: December 2, 2022).
- [37] Daylight and glazing requirements in new construction (no date) Glass For Europe. Glass For Europe. Available at: <https://glassforeurope.com/daylight-and-glazing-requirements-in-new-construction/> (Accessed: December 2, 2022).
- [38] Armstrong, Peter & Dirks, James & Reilly, Raymond & Currie, James & Nesse, Ronald & Komarov, Oleg & Nekrasov, Boris. (2000). Russian Apartment Building Thermal Response Models for Retrofit Selection and Verification. Proceedings, ACEEE Summer Study on Energy Efficiency in Buildings. 3.
- [39] New Buildings in National Residential Building Typologies, 2022. Repository Tufelft. <https://repository.tufelft.nl/islandora/object/uuid:d7ceb03f-699e-4db6-9638-d1db98f8f2f1/datastream/OBJ/download>.
- [40] Building Regulations Update 2022 - YBS Insulation. (2021). YBS Insulation. <http://ybsinsulation.com/building-regulations-update-2022/#:~:text=The%20maximum%20permitted%20U-values,0.15W/m2%20K>.
- [41] What temperature is a heat pump not effective? Easy answer, 2020. linquip. Available at: <https://www.linquip.com/blog/what-temperature-is-a-heat-pump-not-effective/> (Accessed: December 2, 2022).
- [42] Stolworthy, M., 2021. GB Fuel type power generation production. [online] Gridwatch. Available at: <<https://gridwatch.co.uk/>> [Accessed 22 April 2021].
- [43] Department for Business, Energy & Industrial Strategy, 2019. Digest Of UK Energy Statistics (DUKES): Electricity. Digest of UK Energy Statistics (DUKES): annual data. UK Government, pp.1-105.
- [44] Statista, 2020. UK: Total Electricity Consumption 2002-2019 | Statista. [online] Available at: <https://www.statista.com/statistics/322874/electricity-consump>

- tion-from-all-electricity-suppliers-in-the-united-kingdom/ [Accessed 21 April 2021].
- [45] Department for Business, Energy & Industrial Strategy, 2020. UK Energy in Brief 2020. National Statistics. [online] London: UK Government, pp.5-44. Available at: <[https://assets.publishing.service.gov.uk/government/uploads/system/uploads/attachment\\_data/file/904503/UK\\_Energy\\_in\\_Brief\\_2020.pdf](https://assets.publishing.service.gov.uk/government/uploads/system/uploads/attachment_data/file/904503/UK_Energy_in_Brief_2020.pdf)> [Accessed 22 April 2021].
- [46] Milev, G., Al-Habaibeh, A. and Shin, D., 2020. Effect of replacing conventional cars with Electric Vehicles on UK electricity grid and carbon emissions. In: International Conference on Energy and Sustainable Futures (ICESF2020). Hertfordshire: University of Hertfordshire, UK, 10-11 September.
- [47] G. Milev, A. Hastings, A. Al-Habaibeh, The environmental and financial implications of expanding the use of electric cars - A Case study of Scotland, *Energy Built Environ.* 2 (2) (2020) 204–213.
- [48] X. Liu, J. Zhu, J. Wang, Y. Fu, H. Zhang, J. Niu, Zero fluctuation: Electric-fluctuation-elimination heat pump system with water storage tank based on time-of-use tax, *Energ. Buildings* 279 (2023), 112703, <https://doi.org/10.1016/j.enbuild.2022.112703>.
- [49] J. Deng, C. Peng, W. Qiang, Q. Wei, H. Zhang, Can heat pump heat storage system perform better for space heating in China's primary schools? A field test and simulation analysis, *Energ. Buildings* 279 (2023), 112684, <https://doi.org/10.1016/j.enbuild.2022.112684>.
- [50] U. Berardi, S. Jones, The efficiency and GHG emissions of air source heat pumps under future climate scenarios across Canada, *Energ. Buildings* 262 (2022), 112000, <https://doi.org/10.1016/j.enbuild.2022.112000>.
- [51] Energy Saving Trust, 2021. Renewable Heat Incentive scheme - Energy Saving Trust. [online] Available at: <https://energysavingtrust.org.uk/grants-and-loans/renewable-heat-incentive/#:~:text=What%20is%20the%20Renewable%20Heat,heating%20coming%20from%20renewable%20sources>. [Accessed 11 May 2021].